Cell

Four centuries of commercial whaling eroded 11,000 years of population stability in bowhead whales

Graphical abstract

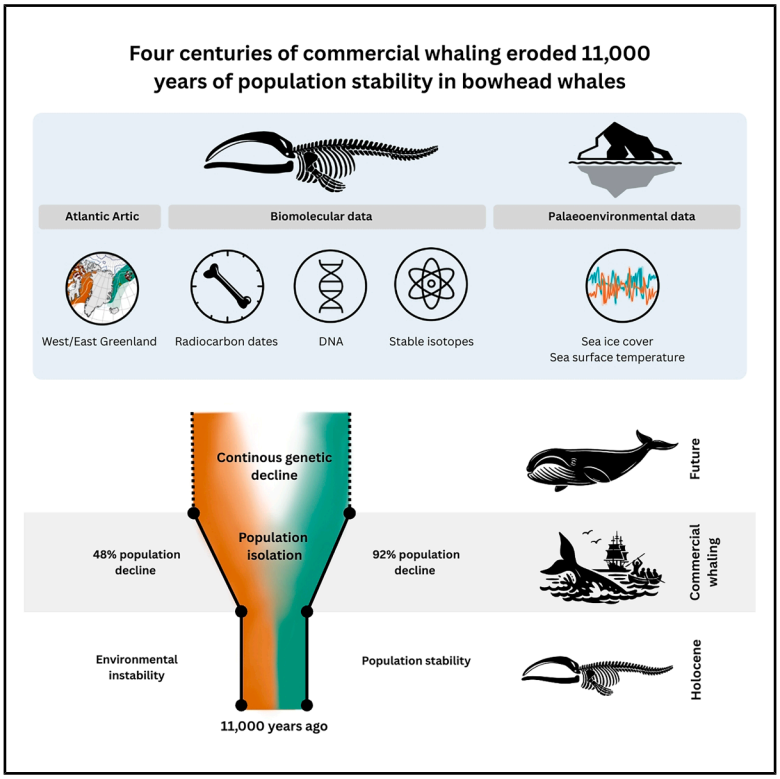

Highlights

- Integrating paleogenomics, stable isotopes, habitat modeling, and paleoclimate data
- Holocene bowhead whales show long-term genomic stability despite environmental change
- Commercial-whaling-driven genetic erosion is ongoing and not yet fully realized
- Even full demographic recovery cannot restore pre-whaling fitness

Authors

Michael V. Westbury, Stuart C. Brown, Andrea A. Cabrera, ..., Paul Szpak, Damien A. Fordham, Eline D. Lorenzen

Correspondence

micwe@dtu.dk (M.V.W.), elinelorenzen@sund.ku.dk (E.D.L.)

In brief

Although bowhead whales remained genetically stable through 11,000 years of Holocene environmental change, commercial whaling upended this long-term stability, driving population subdivision and genomic erosion that are still unfolding today.

Westbury et al., 2026, Cell *189*, 1–14
April 2, 2026
https://doi.org/10.1016/j.cell.2026.02.022

CellPress

Cell

CellPress
OPEN ACCESS

Article

Four centuries of commercial whaling eroded 11,000 years of population stability in bowhead whales

Michael V. Westbury,[1,11,*] Stuart C. Brown,[1,2] Andrea A. Cabrera,[1] Hernán E. Morales,[1] Bárbara Parreira,[1] Jilong Ma,[3] Moisès Coll Macià,[3] Alba Rey-Iglesia,[1] Arthur Dyke,[4] Camilla Hjorth Scharff-Olsen,[1] Michael B. Scott,[5] Øystein Wiig,[6] Lutz Bachmann,[6] Kit M. Kovacs,[7] Christian Lydersen,[7] Steven H. Ferguson,[8] Paul Szpak,[5] Damien A. Fordham,[1,2,9,10] and Eline D. Lorenzen[1,12,*]

[1]Globe Institute, University of Copenhagen, Copenhagen, Denmark
[2]Environment Institute and School of Biological Sciences, University of Adelaide, Adelaide, SA, Australia
[3]Bioinformatics Research Center, Aarhus University, Aarhus, Denmark
[4]Department of Anthropology, McGill University, Montreal, QC, Canada
[5]Department of Anthropology, Trent University, Peterborough, ON, Canada
[6]Natural History Museum, University of Oslo, Oslo, Norway
[7]Norwegian Polar Institute, Fram Center, 9296 Tromsø, Norway
[8]Fisheries and Oceans Canada, Winnipeg, MB, Canada
[9]Center for Macroecology, Evolution and Climate, University of Copenhagen, Copenhagen, Denmark
[10]Center for Global Mountain Biodiversity, University of Copenhagen, Copenhagen, Denmark
[11]Present address: Department of Health Technology, Section for Bioinformatics, Technical University of Denmark, Kongens Lyngby, Denmark
[12]Lead contact
*Correspondence: micwe@dtu.dk (M.V.W.), elinelorenzen@sund.ku.dk (E.D.L.)
https://doi.org/10.1016/j.cell.2026.02.022

SUMMARY

Bowhead whales were heavily exploited during commercial whaling between the 16th and 20th centuries. Current and near-future climate warming poses a new threat. Assessing bowhead vulnerability to climatic change remains challenging due to insufficient knowledge regarding responses to past climates and pre-whaling population dynamics. We integrate paleogenomics and stable isotopes ($\delta^{13}C$ and $\delta^{15}N$) from 206 bowhead fossils from the Atlantic Arctic with paleoclimate and ecological modeling based on 823 radiocarbon-dated fossils, including 140 from this study. We find long-term resilience of bowheads to Holocene environmental perturbations, with no detectable changes in genetic diversity or population structure. Simulated commercial-whaling-driven genetic and fitness changes indicate that population subdivision and loss of genetic diversity are unlikely to be fully realized, despite nearly a century since whaling ceased. Furthermore, even in simulated complete population recovery scenarios, overall fitness did not return to pre-whaling levels, potentially compromising the future resilience of bowhead whales.

INTRODUCTION

Humans have relied on cetacean species to support their livelihoods for millennia, with whale bones being common at many coastal archaeological sites.[1] In the Arctic and subarctic, subsistence harvesting of cetaceans started with the arrival of the pre-contact Inuit culture (Thule) ~1,000 years ago[2] and remains significant to communities across the Arctic today. Bowhead whales (*Balaena mysticetus*)—the only baleen whale found in the Arctic year-round—were harvested relatively heavily by the Thule,[3] who are the ancestors of modern Inupiat and Inuit. The Thule culture emerged in Alaska around 1000 CE and, beginning some time after 1200 CE, spread rapidly eastward, colonizing much of the Canadian Arctic and Greenland.[4] Their subsistence practices varied regionally, but in some areas, such as around Somerset Island, bowhead whales were targeted during the Classic Thule period (~1200–1500 CE).[5]

Levels of Thule harvests of bowhead whales in the central and eastern Canadian Arctic are difficult to estimate but have been approximated at ~11,500 whales landed between 1200 and 1529 CE,[3] roughly 20% of the total commercial harvests that followed. Although the number of bowhead whales taken by the Thule is large, these early hunters mainly targeted non-breeding whales (primarily yearlings).[6] This age-selective harvest is likely to have had limited impact on population growth and, hence, population size. This is because compensatory dynamics, such

Please cite this article in press as: Westbury et al., Four centuries of commercial whaling eroded 11,000 years of population stability in bowhead whales, Cell (2026), https://doi.org/10.1016/j.cell.2026.02.022

as reduced intraspecific competition and natural mortality replacement, can offset the loss of young age classes.[7,8] Thus, major anthropogenic-driven population declines of bowhead whales likely did not occur before the introduction of commercial-scale harvesting in 1540 CE.[9]

The bowhead whale was one of the first whale species to be commercially exploited, beginning with whaling by the Basques in the Strait of Belle Isle in southern Labrador, Canada.[10] After depletion of the whales around Labrador, the hunt moved east to Svalbard (Norway) in 1611 CE,[11,12] and in 1847–1849 CE, commercial whalers started to exploit the North Pacific, both the Sea of Okhotsk and the Bering Sea.[10]

Cumulative offtake (relative to population size) during the four centuries of commercial bowhead whaling is estimated to have been much more severe in the eastern sector of the Atlantic Arctic compared with areas in the western sector.[10] Prior to whaling, the 'East Greenland-Svalbard-Barents Sea' (EGSB) stock numbered in excess of 52,000 bowheads.[12] Currently, this population likely numbers only a few hundred individuals.[12,13] In contrast, a pre-whaling estimate for the 'East Canada-West Greenland' (ECWG) stock is ~18,500 individuals,[14] and the current population numbers ~6,000 individuals.[15]

The main reason for commercial exploitation of bowhead whales was the value of the oil rendered from their blubber, which comprises 45%–55% of the weight of an individual.[16] Whale oil was the main source of light in cities across Europe and the eastern United States until the mid-1800s, when gas and then later petroleum became available.[10] By the early 20th century, when commercial bowhead whaling ceased to be profitable, populations had been driven close to extinction.[10] Bowhead whale protection was put in place in 1931 with the signing of the "Convention for the Regulation of Whaling,"[9] which banned the harvest of all species in the right whale family (Balaenidae).

The decimation of bowhead populations caused by commercial whaling likely had wide-reaching effects, not only via the loss of genetic diversity—and therefore the adaptive potential of bowhead whales themselves—but also on Arctic marine food webs[17] and on Indigenous communities reliant on these ecosystems for subsistence.[18,19] Bowhead whales are a major consumer of copepods and other zooplankton and a keystone species responsible for nutrient cycling in Arctic ecosystems. They live in tight association with sea ice, which provides them with protection from killer whales (*Orcinus orca*)[20] and also provides them with a low-competition environment.[21]

The distribution and genetics of contemporary bowhead populations provide valuable information on present-day levels of population subdivision and genetic diversity.[22–25] Although genetic data from contemporary bowhead whale populations have been used to study the genetic impacts of whaling,[24,26,27] detecting and quantifying population size changes using contemporary data alone is challenging. This is partly because of the long generation times of the species (35–50 years[22]), leading to a slow accumulation of genetic signatures of past demographic events.[28] Thus, the genetic consequences of whaling are unlikely to be fully evident using contemporary data alone.

An accurate representation of long-term, pre-whaling populations is necessary to assess the near-future responses of bowhead whales to a changing Arctic. To predict how bowhead whales will respond to near-future change, we must first understand long-term, baseline patterns of population diversity and subdivision. By examining the impact of past environmental shifts on populations, we can better assess the genomic consequences of commercial whaling. This historical lens is key to evaluating their resilience moving forward.

Previous studies that have used mitochondrial DNA retrieved from ancient and present-day bowhead whales to assess the impacts of past climate change and commercial whaling[29–31] concluded that neither climate nor whaling has left a genetic impact. However, mitochondrial DNA represents just a single maternally inherited locus, raising questions as to whether the data analyzed had the capacity to reveal the genetic effects of these processes. Whole-genomic data, which incorporates thousands of independent loci, provides a more powerful approach to assessing past changes in demography and population relationships.

Bowhead whales have an exceptional—and, in the context of other marine mammals, unprecedented—fossil record. Bowhead whales usually float when dead,[32] and carcasses end up on shore more frequently than is the case for other large cetaceans that tend to sink to depth when they die. Large numbers of bowhead bones discovered on beaches in the Canadian Arctic Archipelago and in the Svalbard Archipelago (Norway) span the past 11,000 years and provide a detailed chronology of bowhead occurrence in these regions. The unprecedented spatial and temporal extent of fossil remains has enabled their use as proxies to estimate the timing and extent of Holocene changes in sea-ice cover, sea level, and glaciation in sectors of the Atlantic Arctic.[33,34]

Using a multi-faceted approach integrating ancient biomolecular analyses (radiocarbon dating, ancient DNA/paleogenomics, and stable isotope [δ^{13}C and δ^{15}N] analysis) with paleoclimate data, ecological models, and genomic simulations, we investigated the past 11,000 years of bowhead whale eco-evolutionary history in the Atlantic Arctic, building on inferences from the exceptional Holocene fossil chronology of 823 radiocarbon-dated fossil remains, of which 140 are from this study (Figure 1). Specifically, we (1) establish a long-term baseline of pre-whaling demographic trends of bowhead whales, (2) elucidate the genomic and paleoecological responses of bowhead whales to Holocene climate change events, and (3) evaluate the future long-term evolutionary impact of commercial whaling on the species.

RESULTS AND DISCUSSION

Holocene environmental changes and habitat suitability

Our high-resolution paleoclimate reconstructions of Holocene environmental change based on the HadCM3B-M2.1 for the Canadian Arctic and Svalbard archipelagos reveal fluctuations in average sea-surface temperature (SST) and sea-ice cover (percentage of the predefined area covered by sea-ice) during the past 11,000 years, with the most dramatic changes occurring around Svalbard (Figures 2A and 2B). We find evidence of

Please cite this article in press as: Westbury et al., Four centuries of commercial whaling eroded 11,000 years of population stability in bowhead whales, Cell (2026), https://doi.org/10.1016/j.cell.2026.02.022

CellPress
OPEN ACCESS

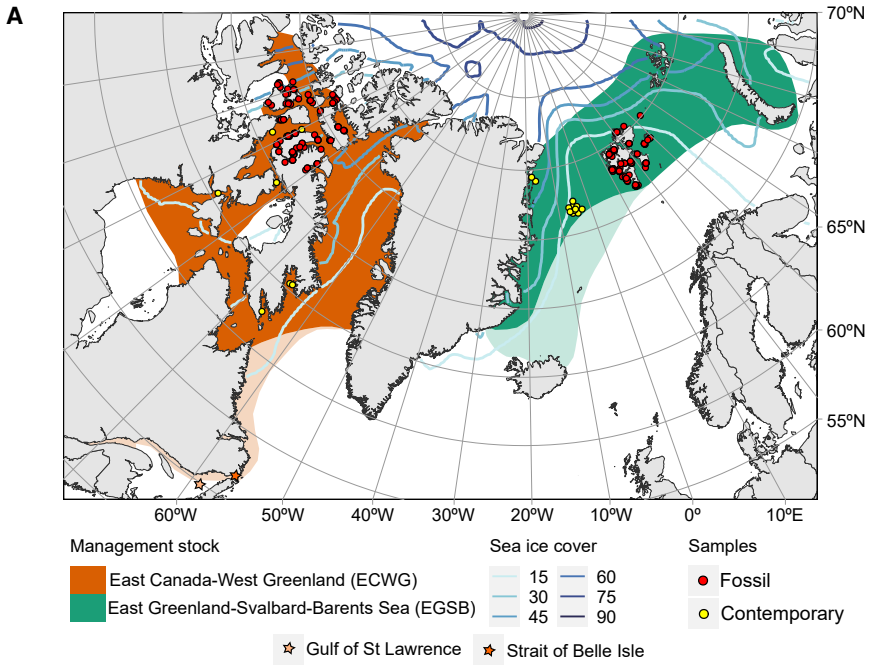

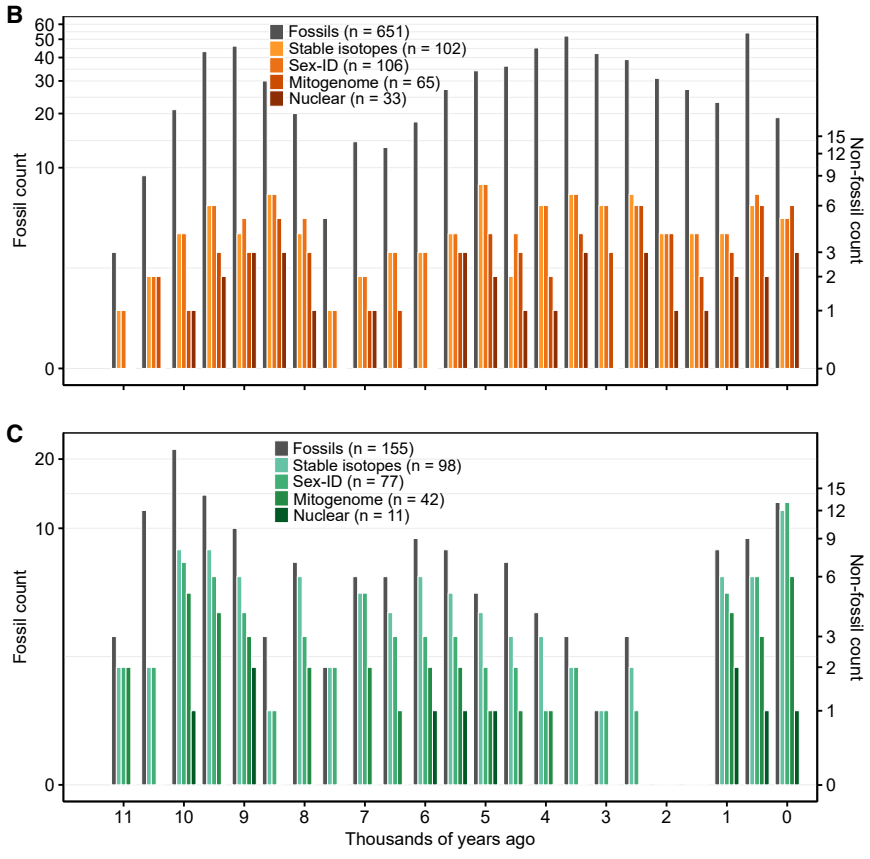

Figure 1. Sample localities and ancient biomolecular data for the Holocene bowhead whale fossil assemblage

(A) Map showing the geographic range of the two recognized bowhead management stocks in the Atlantic Arctic. Faded colors show the historical distribution that was lost after commercial whaling. Current summer sea-ice concentrations across the Arctic Ocean are indicated by blue lines. The locality of the Holocene fossil samples from which we retrieved ancient biomolecular data ($\delta^{13}C$ and $\delta^{15}N$ stable isotopes, ancient DNA) are shown as red dots. Sampling locations of the individuals used to generate the contemporary genomes are shown as yellow dots, and specific geographic localities mentioned in the text are indicated by a star.

(B and C) The complete dataset from (B) the Canadian Arctic Archipelago and (C) the Svalbard Archipelago, including the total number of radiocarbon-dated fossils, stable $\delta^{13}C$ and $\delta^{15}N$ isotopes, and ancient DNA for genetic sexing, nuclear genomes (>0.2× coverage), and mitochondrial genomes (>10× coverage), are shown in 500-year time bins.

correlation between these two variables: $R^2 = 0.62$ for the Canadian Arctic Archipelago and 0.93 for the Svalbard Archipelago (Figure S1; Table S1). The HadCM3B-M2.1 is a specific version of the Hadley Centre's climate model HadCM3, used for simulating climate processes over the past 60,000 years.[35] It shows that the largest shifts in SST and sea-ice cover are likely to have taken place in the early Holocene, with large peaks in SST and troughs in sea-ice cover in the Canadian Arctic Archipelago at ~10–8.5 thousand years ago (kya). This timing roughly coincides with the onset of the Holocene Thermal Maximum[36,37] and the opening of the Nares Strait ~9 kya that connects Baffin Bay and the Lincoln Sea to the Arctic Ocean, flooding the region with nutrient-rich water from the Atlantic.[38]

Differences in the timing of paleoclimatic shifts in the western and eastern sectors of the Atlantic Arctic probably reflect heterogeneity in the timing and duration of the Holocene Thermal Maximum across the Arctic.[37] The rapid decline in SST observed in Svalbard ~6 kya may signal the end of the Holocene Thermal Maximum in the region (Figure 2A). However, despite pronounced early Holocene fluctuations in SST and sea-ice cover, our ecological models do not suggest concurrent changes in the estimated area (Figure 2C) or spatial distribution (measured as average latitude) (Figure 2D) of suitable bowhead whale habitats. Conversely, habitat suitability projections are relatively stable across time (Video S1), with suitable habitat being weakly correlated with SST and sea-ice cover; R^2 values between 0.03 and 0.24

Please cite this article in press as: Westbury et al., Four centuries of commercial whaling eroded 11,000 years of population stability in bowhead whales, Cell (2026), https://doi.org/10.1016/j.cell.2026.02.022

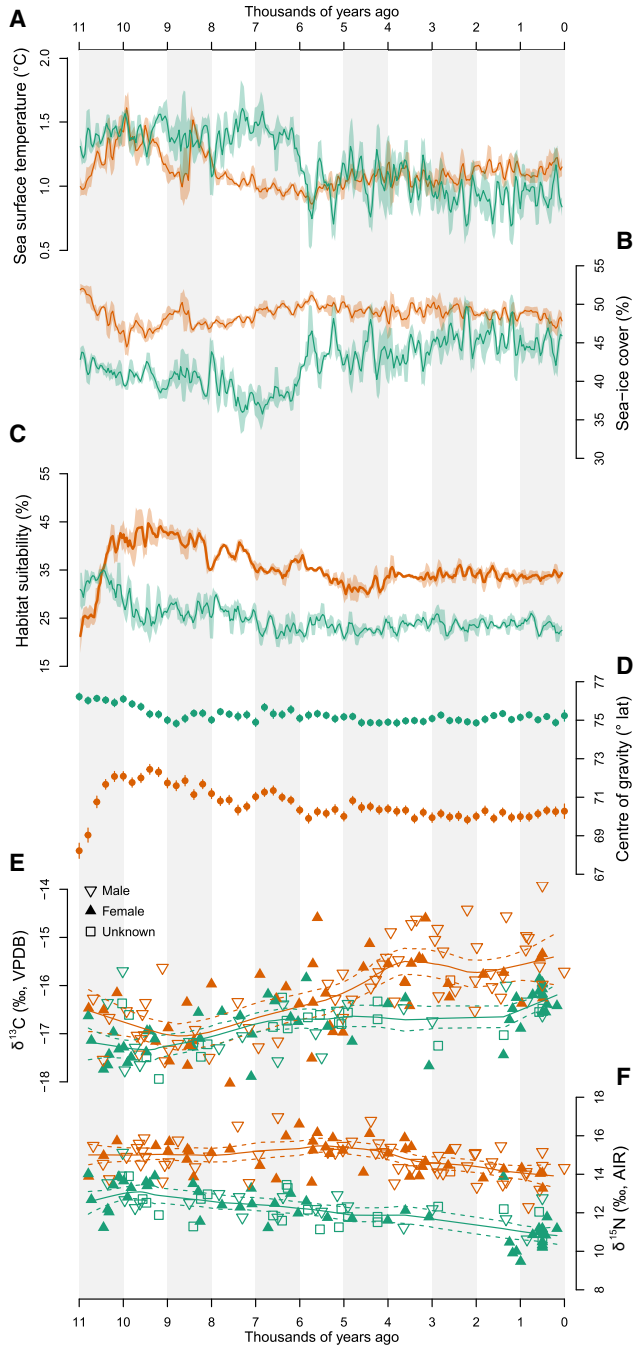

Figure 2. Holocene environmental change, habitat suitability, and paleoecology

(A and B) Holocene (A) SST and (B) percentage of the predefined area covered by sea ice.

(C) Percentage of the predefined area containing suitable habitat for bowhead whales based on our models.

(D–F) (D) Average latitude of suitable habitat within the predefined region. Bone collagen stable (E) $\delta^{13}C$ and (F) $\delta^{15}N$ isotope values from 196 Holocene bowhead whale fossils, and their genetic sex, if available; the specimens included 94 females, 78 males, and 24 individuals for which sex could not be determined. Trend lines are from a local weighted regression smoothed to fit our scatterplot data. Information about the Canadian Arctic Archipelago is shown in orange and that from the Svalbard Archipelago is shown in green.

See also Figures S1 and S3–S5.

(Figure S1; Table S1) suggest a level of resilience of bowhead whale habitat to the climatic perturbations of the Holocene.

In agreement with our continuous spatiotemporal estimates of suitable habitat, we observed limited changes in genetic diversity of bowhead whales across the Holocene, as measured by genome-wide single-nucleotide polymorphism (SNP) heterozygosity and nuclear and mitochondrial nucleotide diversity (π) assessed in 1,000-year time bins (Figures 3A and S2; see extended data figure 1 and tables 1–3 on Zenodo). Correlations between genome-wide SNP heterozygosity and SST and sea-ice cover were low (R^2 values < 0.133) (Figure S3; Table S1). This suggests that Holocene environmental shifts, as identified by changes in SST and sea-ice cover, had negligible impacts on genetic diversity and, presumably, population abundance of bowhead whales. Alternatively, any local changes in genetic diversity were buffered by inter-regional migration and gene flow.

Nevertheless, the apparent long-term stability observed in bowhead whale genetic diversity across the Holocene, despite significant environmental perturbations, is in contrast with other Arctic marine mammals for which Holocene population reconstructions are available. For example, Greenlandic polar bears (*Ursus maritimus*) experienced marked concurrent declines in suitable habitat and in effective population size during the Holocene in response to increasing SST and decreasing sea-ice cover.[39]

Spatiotemporal patterns of bowhead paleoecology

To further investigate the response of bowhead whales to environmental change, we analyzed bone collagen stable carbon ($\delta^{13}C$) and nitrogen ($\delta^{15}N$) isotope compositions from our fossil chronology (Figures 2E and 2F; see extended data figure 2 on Zenodo). These data provide a proxy for assessing temporal shifts in resources at the base of the food web, i.e., in primary productivity or nutrients, which can be driven by climatic and environmental change.[40] Bowhead whales are specialized zooplankton feeders, and thus it is unlikely that they would shift their trophic position during the time investigated by our study. However, sea-ice microalgae, growing within and under sea ice, and phytoplankton, growing in open water, experience regional shifts in community composition and abundance in response to reductions in sea-ice cover and thickness that alter primary production regimes.[41] These shifts at the base of the food web drive bottom-up changes in ecosystem structure and function, affecting pelagic secondary production. Such shifts are reflected in the tissue isotopic and chemical compositions of consumers, including bowhead whales.[42]

Our analysis did not reveal a strong correlation between spatiotemporal changes in bowhead $\delta^{13}C$ or $\delta^{15}N$ signatures and suitable habitat (R^2 < 0.066), although weak correlations between $\delta^{13}C$, $\delta^{15}N$, and both SST (R^2 < 0.22) and sea-ice cover (R^2 < 0.12) were detected (Figures 2, S4, and S5; Table S1). The overall trend in δ isotope values through time was consistent, regardless of the sex of the individual (see extended data figure 2

Please cite this article in press as: Westbury et al., Four centuries of commercial whaling eroded 11,000 years of population stability in bowhead whales, Cell (2026), https://doi.org/10.1016/j.cell.2026.02.022

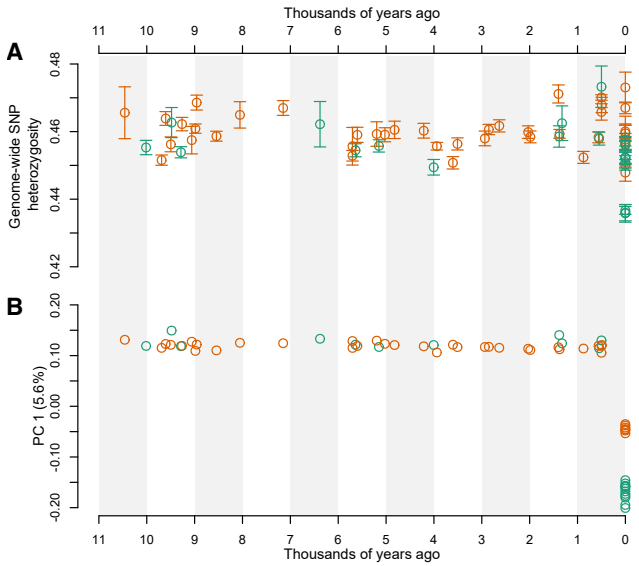

Figure 3. Spatiotemporal patterns of genetic diversity and population subdivision in bowhead whales across 11,000 years

(A) "Corrected" individual genome-wide nuclear SNP heterozygosity. Heterozygosity values were corrected in the Holocene fossil individuals by simulating ancient DNA damage patterns onto contemporary individuals and calculating the deviation from the original, high-quality version of the same individual. Error bars represent one standard deviation from the mean.

(B) The first axis of a PCA, plotted against the age of each sample. The analyses were based on genotype-likelihoods computed from genome-wide data from 44 Holocene fossil individuals with at least 0.2× coverage and 19 contemporary individuals using PCAngsd. A Tracy-Widom test on the eigenvalues showed that only PC1 was significant, $p < 0.01$. Samples from the Canadian Arctic Archipelago are shown in orange (33 pre-whaling Holocene, 7 contemporary). Samples from the Svalbard Archipelago are shown in green (11 pre-whaling Holocene, 12 contemporary). Analyses were performed using a panel of 2,280,657 transversion SNPs.

See also Figures S1 and S3–S5.

on Zenodo). We also did not find any strong correlation ($R^2 < 0.093$) between $\delta^{13}C$ and $\delta^{15}N$ signatures, or between $\delta^{13}C$, $\delta^{15}N$, and genome-wide SNP heterozygosity (Table S1; see extended data figures E3 and E4 on Zenodo). Our findings show similar $\delta^{13}C$ values between the western and eastern sectors of the Atlantic Arctic until ~6 kya, when $\delta^{13}C$ increased in individuals from the Canadian Arctic Archipelago relative to the Svalbard Archipelago. $\delta^{13}C$ values in specimens from the Canadian Arctic Archipelago continued to rise until ~3.5 kya. The timing of the onset of the increase corresponds with the end of the Holocene Thermal Maximum, which may have caused a shift in primary producers as temperatures changed. A similar increase in $\delta^{13}C$ has also been documented in Northwest Greenland in sedimentary organic carbon,[43] suggesting that this pattern is not specific to bowhead whales but rather reflects a regional shift in primary productivity in the western sector of the Atlantic Arctic.

The clear differentiation in $\delta^{15}N$ between bowhead whales from the Canadian Arctic Archipelago and the Svalbard Archipelago is likely due to regional variability in $\delta^{15}N$ at the base of the food web, as has been reported in other marine predators.[39,44,45] During the second half of the Holocene, $\delta^{15}N$ in bowhead whales around both the Canadian Arctic Archipelago and the Svalbard Archipelago decreased gradually (Figure 2F), suggesting a slow change in nutrient dynamics, possibly decreasing rates of sedimentary denitrification, a process that results in ^{15}N-enrichment in water column organic matter in Arctic and subarctic continental shelf environments.[46] Such a change would be reflected in the $\delta^{15}N$ of consumers, such as bowhead whales.[47]

Spatiotemporal patterns of genomic structuring

Bowhead populations are recognized by the International Whaling Commission (IWC) as comprising four geographically segregated stocks, based on genetics and non-genetic data, including telemetry.[48] Contemporary bowhead whales in the Canadian Arctic Archipelago belong to the ECWG stock (Figure 1A). Contemporary bowhead whales from around the Svalbard Archipelago belong to the EGSB stock. Bowhead whales regularly travel within their respective management stock boundaries during the year.

Our F_{ST} analysis shows that the level of genetic differentiation between the two stocks is ~3.7× higher at present than during the Holocene (0.0018 vs. 0.007). Although overall low, this indicates a greater level of population subdivision between contemporary stocks than in the past (see extended data figure 5 on Zenodo). Indeed, our principal-component analysis (PCA) found no indications of genomic population subdivision in our fossil individuals, suggesting that bowhead whales comprised a single panmictic population during the Holocene (Figure 3B; see extended data figures 6–11 on Zenodo). However, regional differences in $\delta^{15}N$ values suggest that whales primarily fed locally, in areas corresponding to where their fossils were found (Figure 2F). Although this points to some degree of geographic segregation in foraging behavior, the lack of genetic structure in the past indicates that gene flow between regions persisted throughout the Holocene. This apparent contrast likely reflects the different timescales captured by genetic vs. isotopic data: while stable isotopes reflect short-term (decades), individual-level foraging behavior, genomic data integrate signals over many generations and are therefore more sensitive to long-term gene flow. Even infrequent interbreeding is likely sufficient to maintain genetic homogeneity, as our evolutionary simulations suggested that the introduction of just one migrant per generation can counteract genetic drift and prevent population divergence.

Our simulations show that a lack of post-whaling migration between stocks could still result in the genetic differentiation patterns we see in our empirical data (Figure 4). This finding is in contrast with what is known about contemporary stocks, as no migration between regions has been recorded.[49–51] Our ecological modeling also supported a scenario of sustained Holocene connectivity between the western and eastern sections of the Atlantic Arctic; we found a high likelihood of suitable habitat around both northern and southern Greenland, connecting the Canadian Arctic Archipelago and the Svalbard Archipelago from 11,000 years ago until 1950 (the most recent time point in our models) (Video S1). The potential for connectivity via paths north of Greenland is supported by fossil evidence of bowhead whales in the far north of Greenland during the Holocene

Please cite this article in press as: Westbury et al., Four centuries of commercial whaling eroded 11,000 years of population stability in bowhead whales, Cell (2026), https://doi.org/10.1016/j.cell.2026.02.022

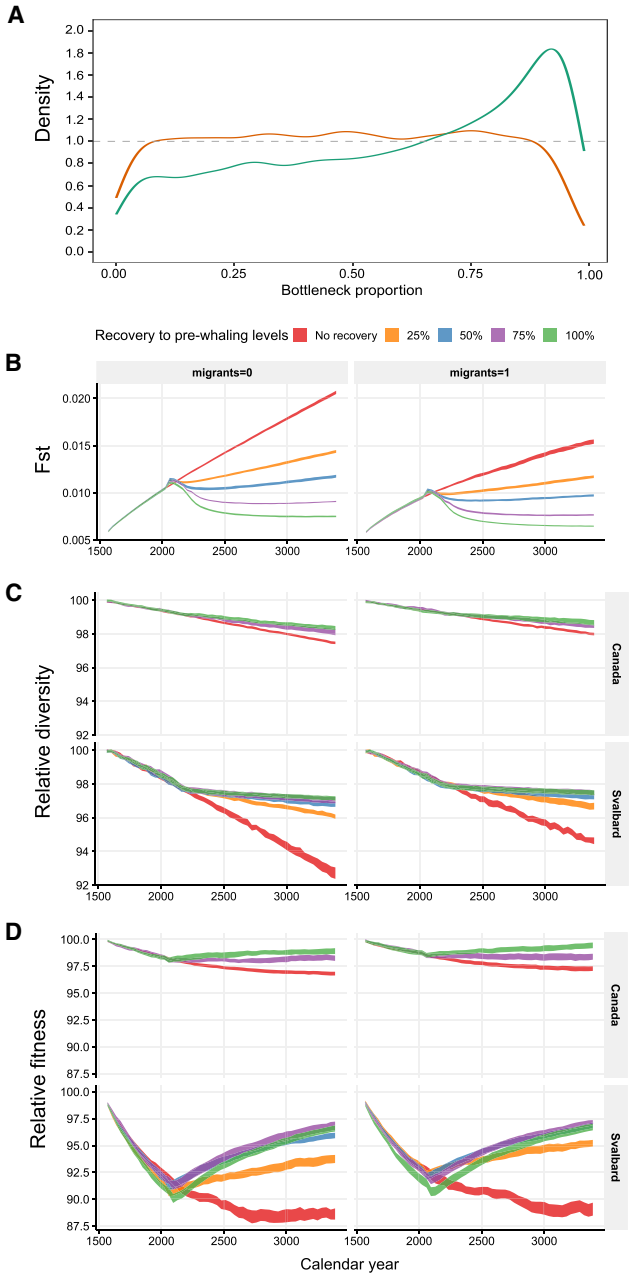

Figure 4. ABC results and simulated impact of commercial whaling based on different recovery scenarios to percentages of pre-whaling levels

(A) ABC results. Colored lines represent the posterior distribution of the simulated populations representing the Canadian Arctic Archipelago (orange) and the Svalbard Archipelago (green) under various population bottleneck proportions. The dashed line represents the prior distribution.

(B–D) Simulated future projections, based on different recovery and migration scenarios: (B) changes in F_{ST} between the two populations; (C) changes in diversity (genome-wide heterozygosity) within the Canadian Arctic Archipelago and Svalbard Archipelago populations; and (D) changes in fitness within the Canadian Arctic Archipelago and Svalbard Archipelago populations. Fitness was calculated by converting realized genetic load to mean population fitness as e^{-RL}, following Bertorelle et al.[52] Simulated bottleneck scenarios included the population representing the Canadian Arctic Archipelago decreasing by 48%, the population representing the Svalbard Archipelago decreasing by 92%, and migration between the populations either ceasing (migrants = 0 per generation) or continuing at the same level as pre-bottleneck (migrants = 1 per generation) after the bottleneck. Plots start at the onset of the simulated commercial whaling bottleneck ~525 years ago. Recovery scenario to 25% of the pre-whaling population size for the Canadian Arctic Archipelago was left out, as the simulated population only decreased to 48% of the pre-whaling size.

(Video S1). As our models are based on summer-suitable habitat, it can be assumed that there were higher levels of suitable habitat around southern Greenland during the winter, which could have facilitated connectivity. Although there is no fossil evidence from southern Greenland, this may be due to the acidity of substrates in the region, which likely limits preservation of organic material, potentially masking the presence of bowhead whales.

The genomic impacts of commercial whaling

At the onset of commercial whaling, the range of bowhead whales extended south of their current winter range in northern Labrador, Canada (Figure 1A).[53] Their range included the Strait of Belle Isle and the Gulf of St. Lawrence, which were the first areas where bowhead whales were heavily hunted by Basque whalers.[10] Their current absence from these areas can be explained by the extirpation of bowhead whales from the southern parts of their range due to early commercial harvests.[10] However, it could also be explained by a reversal of the relative southward displacement of bowhead whales during the cooler climates of the Little Ice Age (~1300–1900 CE). Nevertheless, the extirpation of bowhead whales from this area may have caused a disruption in connectivity between contemporary stocks relative to their pre-whaling counterparts (Figure 3B).

During the four centuries of commercial bowhead whaling, the cumulative harvests in the eastern sector of the Atlantic Arctic are estimated to have been much more severe than in the western sector.[10] Estimates based on whaling records suggest a >98% population size reduction in the east[12,13] and an ~70% population size decline in the west.[14,15] The difference in whaling intensity between regions is mirrored in our dataset; contemporary EGSB individuals have significantly lower mean genome-wide SNP heterozygosity and lower genome-wide nucleotide diversity compared with Holocene individuals (our analysis suggests ~2% loss between pre- and post-whaling individuals for each estimated metric) (Figure 3A; see extended data figure 1 and tables 1–3 on Zenodo). In contrast, contemporary bowhead whales from the ECWG stock have diversity values that do not significantly differ from Holocene individuals from the Canadian Arctic Archipelago, indicating that they more closely reflect pre-whaling diversity than their Svalbard counterparts.

The genetic impact of whaling is also visible to some degree in the genomes of individuals from the contemporary EGSB stock. Our demographic inference, using only the 12 contemporary individuals, estimated an ~12% loss in effective population size (N_e) ~ 5 generations ago, which is equivalent to 250–175 years ago, assuming a generation time of 35–50 years[22] (see extended data figure 12 on Zenodo). Similar findings were recently

reported in bowhead whales in the ECWG stock, which showed a large decrease in $N_e \sim 4$ generations ago.[25] However, demographic reconstruction based exclusively on contemporary genetic data can be challenging, as inferences of past population size changes are indirect and may be hindered by long generation times, short bottleneck duration, and population structure.[54] Thus, long-term, pre-whaling data are imperative for reliably quantifying the relative and long-term genetic impact of commercial whaling.

To estimate the most probable magnitude of the bottleneck caused by commercial whaling, we compared our empirical estimates of spatiotemporal changes in genetic diversity and F_{ST} (Figures 3A and S2; see extended data figure 5 on Zenodo) with genomic simulations of various demographic scenarios in an approximate Bayesian computation (ABC) framework (Figure 4A). The prior distribution for the magnitude of the bottleneck in the Canadian Arctic Archipelago did not differ from the posterior. This means we could not accurately estimate the bottleneck size required to maintain genetic diversity, as observed in the empirical dataset. In other words, the Canadian population could have actually experienced any of our potential scenarios, from no bottleneck to strong declines, as reductions in N_e often leave weak or delayed genetic signatures that may not be detectable over short timescales.[28] Using a model of a 2% relative reduction in genetic diversity in a population modeled after our pre-whaling Svalbard Archipelago population, we estimate that the most probable population decline was approximately 92%.

Using forward evolutionary simulations, we show that population divergence and loss of genetic diversity associated with commercial whaling are not yet fully realized in contemporary populations (Figures 4B and 4C), likely due to the long generation time of bowhead whales and the relatively recent timing of their population bottleneck. The relative diversity of contemporary bowhead whales underestimates the actual loss due to whaling, which ceased in both regions less than ~5 generations ago.[10] Thus, it will likely take several more generations for the genetic signs of low population size to become evident. This is not unexpected, as loss of genetic diversity has a time-lag relative to demographic decline, particularly in long-lived species.[28] Genetic diversity loss in collapsed populations (e.g., Svalbard Archipelago) is expected to continue, even if there is demographic recovery,[55,56] as small populations continue to pay a "genetic drift debt."[57]

Simulations incorporating different population recovery scenarios showed that, even in the best-case scenario, in which both populations rebounded to their original pre-whaling sizes (100% recovery), population differentiation would remain elevated and genetic diversity would continue to decrease over the next ~1,000 years (Figures 4B and 4C), albeit at different rates depending on the recovery scenario. However, our findings indicate that fitness recovers as demography recovers (Figure 4D), likely because selection is effective at removing some of the accumulated genetic load. Despite this, genetic load and loss of fitness will likely never return to pre-whaling levels within our simulated time frame, up to the year 3500 CE, potentially leaving bowhead whales permanently less robust than they were prior to commercial whaling.

Our finding of sustained genomic erosion, especially in the EGSB stock, brings into question the long-term resilience of the population. Although fitness may recover as selection removes deleterious variants, the ongoing loss of genome-wide diversity threatens their adaptive potential in response to future environmental change. This depends on the available additive genetic variance, which genetic drift reduces in collapsed populations.[55] Genome-wide diversity is a key predictor of both population viability and adaptive potential.[58,59] Beyond limiting evolutionary potential, the loss of genome-wide diversity can also erode immunogenetic variation,[60] leaving collapsed populations more susceptible to emerging diseases. The loss of genetic diversity will likely be exacerbated by further declines in population size, which are predicted based on modeled future patterns of habitat suitability, showing a significant decrease and northward shift toward 2100 CE.[61,62] Overall, our findings highlight the pressing need for long-term protection and (genetic) monitoring of bowhead whale populations.

The relative impact of commercial whaling

Prior to commercial whaling, bowhead whales in the western sector of the Atlantic Arctic endured hundreds of years of Palaeoinuit subsistence hunting. The average harvests translate to ~40 individuals per year for Thule subsistence harvests and ~150 individuals per year for commercial harvests. However, there was a relatively short, concentrated period of significantly higher commercial takes in eastern Canada and West Greenland, of up to 1,500 individuals per year between ~1830 and 1840 CE.[3]

Based on the size of bones retrieved from archaeological sites, Thule are inferred to have focused almost exclusively on non-breeding individuals (yearlings and small juveniles)[6] and thus likely had lower impacts on the species relative to commercial whaling, which was either non-selective or targeted the largest animals.[63] Indeed, a negligible impact of Indigenous whaling is supported by our findings, which show no evidence of genetic diversity loss prior to commercial whaling (Figure 3). The longer period of sustained bowhead harvests in the Canadian Arctic Archipelago by Thule and commercial whalers, relative to Svalbard, where there have never been subsistence harvests, makes the regional patterns of diversity loss in contemporary individuals all the more profound; our data show that commercial exploitation left the Svalbard whales in a much worse state than their Canadian counterparts, in agreement with regional differences in harvest estimates.[10]

The Arctic is experiencing transformative change due to climate warming. The region is experiencing a 4-fold amplification of the rate of change in temperature compared with the global average.[64] Climate models predict further increases in SST and losses of sea-ice cover in our two study regions in the near future[61,62] (see extended data tables 4 and 5 on Zenodo). Although some climatic perturbations at the Pleistocene/Holocene transition were similar in pace and magnitude to what is predicted for the 21st century,[65] absolute temperatures in the Arctic this century are predicted to exceed those experienced during the past 55 million years.[66,67] We show that bowhead whales across the Atlantic

Arctic are likely to have been resilient to the past 11,000 years of environmental perturbations. Our results indicate that higher levels of nuclear genetic diversity and higher potential for gene flow during the Holocene could have promoted genetic and demographic stability in the face of past environmental change. However, our study indicates that the impacts of commercial whaling are driving population subdivision and eroding genetic diversity and that we have yet to see the full genomic consequences of the commercial decimation of bowhead populations, which may impact the species' resilience to near-future climate change.

Bowhead whales are a sentinel species for elucidating the impacts of environmental changes on Arctic marine ecosystems.[68] The exceptional bowhead whale fossil record—unique at a global scale—provides a window into 11,000 years of bowhead whale eco-evolutionary history and, by extension, the short-chained food web of which they are a part. Our approach integrates radiocarbon dating, genomic data, stable isotope analysis, ecological modeling, and simulations, providing a solid framework for investigating long-term ecosystem response to climate change and anthropogenic pressures. By linking past environmental changes with species-specific responses, our findings illustrate how anthropogenic pressures have disrupted thousands of years of ecosystem stability. This underscores the profound and lasting impact of human activities on Arctic biodiversity and highlights the urgency of understanding how historical disruptions shape the resilience of ecosystems today and into the future.

Limitations of the study

Despite the comprehensive nature of our multi-proxy approach, there are inherent limitations in our study. Although the integration of radiocarbon dating, paleogenomics, stable isotope, and habitat modeling data provides considerable baseline insight into long-term bowhead whale eco-evolutionary dynamics, it is possible that physiological or behavioral traits that are not visible in the fossil record, or recoverable through ancient biomolecules, may have changed in bowhead whales to cope with past changes in the environment. Relatively little is known about the current genetic health and demography of contemporary bowhead populations, particularly around Svalbard, which makes it difficult to incorporate present-day population status into future genomic simulations. Due to the low coverage and damaged nature of paleogenomic data, we employed a filtered SNP panel for our heterozygosity estimates; although this enables robust relative comparisons within our dataset, these values are not directly comparable to previously published studies using different methodologies or datasets. Furthermore, our finding of long-term stability in habitat suitability is conditional on the spatial resolution of the paleoclimate simulations and ecological models employed. The resolution ($1^\circ \times 1^\circ$ latitude/longitude) reflects the limits of currently available data for long-term paleo reconstructions, and it is possible that finer-scale analyses could reveal more pronounced local changes or shorter-term fluctuations in suitable bowhead whale habitat. Lastly, because bowhead whale distribution and movements can differ markedly between summer and winter, our use of summer data for ecological modeling may underestimate the complexity of their year-round habitat use. This consideration is particularly relevant in the context of historic panmixia, as southward winter movements could have further facilitated inter-population breeding and gene flow during the Holocene.

RESOURCE AVAILABILITY

Lead contact

Further information and requests for resources and reagents should be directed to and will be fulfilled by the lead contact, Eline D. Lorenzen (elinelorenzen@sund.ku.dk).

Materials availability

This study did not generate any new unique reagents.

Data and code availability

Raw genomic sequencing data are available at NCBI Bioproject ID PRJNA1174153, and code for the ecological models can be found at DOI: https://doi.org/10.17605/osf.io/gbxsy. Additional supplementary figures and tables (Extended data figures 1–24 and Extended data tables 1–9) have been deposited on Zenodo and are available at DOI: https://doi.org/10.5281/zenodo.17660988.

ACKNOWLEDGMENTS

We thank the museums—in particular, the Canadian Museum of Nature (CMN), the Natural History Museum Oslo (NHMO), and the University Museum Bergen—and the many sample collectors (incl. Anne Karin Hufthammer, Mads Peter Heide-Jørgensen, and Erik Born), whose continued efforts in collecting, curating, and preserving fossil bowhead whale specimens from the past for the future have enabled this study. We thank Otto Salvigsen (deceased) for the use of unpublished datings from Svalbard. We thank Margaret Currie for her help in finding and sampling the bowhead specimens from the Canadian Museum of Nature and Nicholas Freymueller for helping us navigate the bowhead whaling literature. This study was supported by the Independent Research Fund Denmark Natural Sciences Forskningsprojekt 1 (8021-00218B), Sapere Aude (9064-00025B), the Villum Fonden Young Investigator Programme (13151 and 37352), and EliteForsk-prize 2023 to E.D.L. M.V.W. was supported by a Novo Nordisk Emerging Investigator grant #NNF24SA0093839. A.A.C. was funded by the Rubicon-NWO (project 019.183EN.005). Contemporary bowhead sample collections from Svalbard were funded by the Norwegian Polar Institute, with grants from the Russian-Norwegian Environment Commission and the Norwegian Research Council ICE-whales programme (244488/E10). Radiocarbon dating of fossils from Svalbard and Greenland were partly funded by the Nordisk Ministerråd (grant no. 661045-20201) and the Research Council of Norway (grant nos. 153028/S40 and 146515/420) to NHMO, as well as the Strategic University Program "National Centre for Biosystematics" (grant no. 146515/420), cofunded by the Research Council of Norway and the NHMO.

AUTHOR CONTRIBUTIONS

Conceptualization, M.V.W. and E.D.L.; formal analysis, M.V.W., S.C.B., H.E.M., A.A.C., B.P., J.M., and M.C.M.; investigation, M.V.W., A.R.-I., C.H.S.-O., M.B.S., and P.S.; visualization, M.V.W., S.C.B., and E.D.L.; writing – original draft, M.V.W. and E.D.L.; writing – review and editing, all authors; funding acquisition, E.D.L.; resources, A.D., Ø.W., L.B., K.M.K., C.L., S.H.F., and E.D.L.; data curation, M.V.W., S.C.B., A.A.C., A.D., and Ø.W.; supervision, P.S., D.A.F., and E.D.L.

DECLARATION OF INTERESTS

The authors declare no competing interests.

STAR★METHODS

Detailed methods are provided in the online version of this paper and include the following:

- KEY RESOURCES TABLE
- EXPERIMENTAL MODEL AND STUDY PARTICIPANT DETAILS
  - Bowhead samples
- METHOD DETAILS
  - Ecological niche modelling
  - Stable isotope analysis
  - Genomics
- QUANTIFICATION AND STATISTICAL ANALYSIS

SUPPLEMENTAL INFORMATION

Supplemental information can be found online at https://doi.org/10.1016/j.cell.2026.02.022.

Received: May 15, 2024
Revised: August 18, 2025
Accepted: February 23, 2026

REFERENCES

1. Savelle, J.M., and Kishigami, N. (2013). Anthropological research on whaling: prehistoric, historic and current contexts. Senri Ethnol. Stud. *84*, 1–48.
2. Douglas, M.S.V., Smol, J.P., Savelle, J.M., and Blais, J.M. (2004). Prehistoric Inuit whalers affected Arctic freshwater ecosystems. Proc. Natl. Acad. Sci. USA *101*, 1613–1617. https://doi.org/10.1073/pnas.0307570100.
3. Higdon, J.W. (2010). Commercial and subsistence harvests of bowhead whales (Balaena mysticetus) in eastern Canada and West Greenland. J. Cetacean Res. Manag. *11*, 185–216. https://doi.org/10.47536/jcrm.v11i2.623.
4. Friesen, T.M., and Arnold, C.D. (2008). The timing of the Thule migration: New dates from the western Canadian Arctic. Am. Antiq. *73*, 527–538. https://doi.org/10.1017/S0002731600046850.
5. Savelle, J.M. (2010). Cumulative bowhead whale (Balaena mysticetus) harvest estimates by prehistoric Thule Inuit in the Canadian Arctic 1200–1500 AD: Implications for bowhead whale population modeling and Thule demography. Bull. Nat. Mus. Ethnol *34*, 593–618.
6. Savelle, J.M., and McCartney, A.P. (2012). Thule Eskimo bowhead whale interception strategies. In Arctic Archaeology (Routledge), pp. 437–451.
7. Milner, J.M., Nilsen, E.B., and Andreassen, H.P. (2007). Demographic side effects of selective hunting in ungulates and carnivores. Conserv. Biol. *21*, 36–47. https://doi.org/10.1111/j.1523-1739.2006.00591.x.
8. Milner, J.M., Bonenfant, C., and Mysterud, A. (2011). Hunting Bambi—evaluating the basis for selective harvesting of juveniles. Eur. J. Wildl. Res. *57*, 565–574. https://doi.org/10.1007/s10344-010-0466-x.
9. Tønnessen, J.N., and Johnsen, A.O. (1982). The History of Modern Whaling (University of California Press). https://doi.org/10.1525/9780520418752.
10. Thewissen, J.G.M., and George, J.C. (2021). Commercial whalingChapter 33. In The Bowhead Whale, J.C. George and J.G.M. Thewissen, eds. (Academic Press), pp. 537–547. https://doi.org/10.1016/B978-0-12-818969-6.00033-9.
11. Woodby, D.A., and Botkin, D.B. (1993). Stock sizes prior to commercial whaling. In The Bowhead Whale (Allen Press), pp. 387–407.
12. Allen, R.C., and Keay, I. (2006). Bowhead Whales in the Eastern Arctic, 1611–1911: Population Reconstruction with Historical Whaling. Environ. Hist. *12*, 89–113. https://doi.org/10.3197/096734006776026791.
13. Biddlecombe, B.A., Ferguson, S.H., Heide-Jørgensen, M.P., Gillis, D.M., and Watt, C.A. (2023). Estimating abundance of Eastern Canada-West Greenland bowhead whales using genetic mark-recapture analyses. Glob. Ecol. Conserv. *45*, e02524. https://doi.org/10.1016/j.gecco.2023.e02524.
14. Higdon, J.W., and Ferguson, S.H. (2016). Historical Abundance of Eastern Canada-West Greenland (EC-WG) Bowhead Whales (Balaena mysticetus) Estimated Using Catch Data in a Deterministic Discrete-Time Logistic Population Model (Fisheries and Oceans Canada, Ecosystems and Oceans Science).
15. Givens, G.H., and Heide-Jørgensen, M.P. (2021). Abundance. In The Bowhead Whale, J.C. George and J.G.M. Thewissen, eds. (Elsevier), pp. 77–86. https://doi.org/10.1016/B978-0-12-818969-6.00006-6.
16. George, J.C., Druckenmiller, M.L., Laidre, K.L., Suydam, R., and Person, B. (2015). Bowhead whale body condition and links to summer sea ice and upwelling in the Beaufort Sea. Prog. Oceanogr. *136*, 250–262. https://doi.org/10.1016/j.pocean.2015.05.001.
17. Savoca, M.S., Czapanskiy, M.F., Kahane-Rapport, S.R., Gough, W.T., Fahlbusch, J.A., Bierlich, K.C., Segre, P.S., Di Clemente, J., Penry, G.S., Wiley, D.N., et al. (2021). Baleen whale prey consumption based on high-resolution foraging measurements. Nature *599*, 85–90. https://doi.org/10.1038/s41586-021-03991-5.
18. Sørensen, M., and Gulløv, H.C. (2012). The Prehistory of Inuit in Northeast Greenland. Arct. Anthropol. *49*, 88–104. https://doi.org/10.1353/arc.2012.0016.
19. Gulløv, H.C., Pedersen, J.B.T., Jakobsen, B.H., and Kroon, A. (2010). Commercial hunting activities in the Greenland Sea: The impact of the European blubber industry on East Greenland Inuit societies/Optically Stimulated Luminescence dating of Inuit settlement structures in coastal landscapes of Northeast Greenland. Geogr. Tidsskr. Dan. J. Geogr. *110*, 357–371. https://doi.org/10.1080/00167223.2010.10669516.
20. Matthews, C.J.D., Breed, G.A., LeBlanc, B., and Ferguson, S.H. (2020). Killer whale presence drives bowhead whale selection for sea ice in Arctic seascapes of fear. Proc. Natl. Acad. Sci. USA *117*, 6590–6598. https://doi.org/10.1073/pnas.1911761117.
21. Ashjian, C.J., Campbell, R.G., and Okkonen, S.R. (2021). Biological environmentChapter 26. In The Bowhead Whale, J.C. George and J.G.M. Thewissen, eds. (Academic Press), pp. 403–416. https://doi.org/10.1016/B978-0-12-818969-6.00026-1.
22. Cerca, J., Westbury, M.V., Heide-Jørgensen, M.P., Kovacs, K.M., Lorenzen, E.D., Lydersen, C., Shpak, O.V., Wiig, Ø., and Bachmann, L. (2022). High genomic diversity in the endangered East Greenland Svalbard Barents Sea stock of bowhead whales (Balaena mysticetus). Sci. Rep. *12*, 6118. https://doi.org/10.1038/s41598-022-09868-5.
23. Rooney, A.P., Honeycutt, R.L., and Derr, J.N. (2001). Historical population size change of bowhead whales inferred from DNA sequence polymorphism data. Evolution *55*, 1678–1685. https://doi.org/10.1111/j.0014-3820.2001.tb00687.x.
24. Phillips, C.D., Hoffman, J.I., George, J.C., Suydam, R.S., Huebinger, R.M., Patton, J.C., and Bickham, J.W. (2012). Molecular insights into the historic demography of bowhead whales: understanding the evolutionary basis of contemporary management practices. Ecol. Evol. *3*, 18–37. https://doi.org/10.1002/ece3.374.
25. de Greef, E., Müller, C., Thorstensen, M.J., Ferguson, S.H., Watt, C.A., Marcoux, M., Petersen, S.D., and Garroway, C.J. (2024). Unraveling the genetic legacy of commercial whaling and population dynamics in arctic bowhead whales and narwhals. Glob. Chang. Biol. *30*, e17528. https://doi.org/10.1111/gcb.17528.
26. Bachmann, L., Cabrera, A.A., Heide-Jørgensen, M.P., Shpak, O.V., Lydersen, C., Wiig, Ø., and Kovacs, K.M. (2020). Mitogenomics and the genetic differentiation of contemporary Balaena mysticetus (Cetacea) from Svalbard. Zool. J. Linn. Soc. *191*, 1192–1203.
27. Rooney, A.P., Honeycutt, R.L., Davis, S.K., and Derr, J.N. (1999). Evaluating a putative bottleneck in a population of bowhead whales from

patterns of microsatellite diversity and genetic disequilibria. J. Mol. Evol. *49*, 682–690. https://doi.org/10.1007/PL00006589.

28. Gargiulo, R., Budde, K.B., and Heuertz, M. (2025). Mind the lag: understanding genetic extinction debt for conservation. Trends Ecol. Evol. *40*, 228–237. https://doi.org/10.1016/j.tree.2024.10.008.

29. Borge, T., Bachmann, L., Bjørnstad, G., and Wiig, O. (2007). Genetic variation in Holocene bowhead whales from Svalbard. Mol. Ecol. *16*, 2223–2235. https://doi.org/10.1111/j.1365-294X.2007.03287.x.

30. Foote, A.D., Kaschner, K., Schultze, S.E., Garilao, C., Ho, S.Y.W., Post, K., Higham, T.F.G., Stokowska, C., van der Es, H., Embling, C.B., et al. (2013). Ancient DNA reveals that bowhead whale lineages survived Late Pleistocene climate change and habitat shifts. Nat. Commun. *4*, 1677. https://doi.org/10.1038/ncomms2714.

31. McLeod, B.A., Frasier, T.R., Dyke, A.S., Savelle, J.M., and White, B.N. (2012). Examination of ten thousand years of mitochondrial DNA diversity and population demographics in bowhead whales (Balaena mysticetus) of the Central Canadian Arctic. Mar. Mamm. Sci. *28*, E426–E443. https://doi.org/10.1111/j.1748-7692.2011.00551.x.

32. Savelle, J.M., Dyke, A.S., and McCartney, A.P. (2000). Holocene Bowhead Whale (Balaena mysticetus) Mortality Patterns in the Canadian Arctic Archipelago. Arctic *53*, 414–421. https://doi.org/10.14430/arctic871.

33. Dyke, A.S., Hooper, J., and Savelle, J.M. (1996). A History of Sea Ice in the Canadian Arctic Archipelago Based on Postglacial Remains of the Bowhead Whale (Balaena mysticetus). Arctic *49*, 235–255. https://doi.org/10.14430/arctic1200.

34. Salvigsen, O., and Slettemark, Ø. (1995). Past glaciation and sea levels on Bjørnøya, Svalbard. Polar Res. *14*, 245–251. https://doi.org/10.3402/polar.v14i2.6666.

35. Valdes, P.J., Armstrong, E., Badger, M.P.S., Bradshaw, C.D., Bragg, F., Crucifix, M., Davies-Barnard, T., Day, J.J., Farnsworth, A., Gordon, C., et al. (2017). The BRIDGE HadCM3 family of climate models: HadCM3@Bristol v1.0. Geosci. Model Dev. *10*, 3715–3743. https://doi.org/10.5194/gmd-10-3715-2017.

36. Axford, Y., de Vernal, A., and Osterberg, E.C. (2021). Past Warmth and Its Impacts During the Holocene Thermal Maximum in Greenland. Annu. Rev. Earth Planet. Sci. *49*, 279–307. https://doi.org/10.1146/annurev-earth-081420-063858.

37. Kaufman, D.S., Ager, T.A., Anderson, N.J., Anderson, P.M., Andrews, J.T., Bartlein, P.J., Brubaker, L.B., Coats, L.L., Cwynar, L.C., Duvall, M.L., et al. (2004). Holocene thermal maximum in the western Arctic (0–180°W). Quat. Sci. Rev. *23*, 529–560. https://doi.org/10.1016/j.quascirev.2003.09.007.

38. Jennings, A., Sheldon, C., Cronin, T., Francus, P., Stoner, J., and Andrews, J. (2011). The Holocene history of Nares strait: Transition from glacial bay to arctic-Atlantic throughflow. Oceanography *24*, 26–41. https://doi.org/10.5670/oceanog.2011.52.

39. Westbury, M.V., Brown, S.C., Lorenzen, J., O'Neill, S., Scott, M.B., McCuaig, J., Cheung, C., Armstrong, E., Valdes, P.J., Samaniego Castruita, J.A., et al. (2023). Impact of Holocene environmental change on the evolutionary ecology of an Arctic top predator. Sci. Adv. *9*, eadf3326. https://doi.org/10.1126/sciadv.adf3326.

40. Szpak, P., Savelle, J.M., Conolly, J., and Richards, M.P. (2019). Variation in late holocene marine environments in the Canadian Arctic Archipelago: Evidence from ringed seal bone collagen stable isotope compositions. Quat. Sci. Rev. *211*, 136–155. https://doi.org/10.1016/j.quascirev.2019.03.016.

41. Lannuzel, D., Tedesco, L., van Leeuwe, M., Campbell, K., Flores, H., Delille, B., Miller, L., Stefels, J., Assmy, P., Bowman, J., et al. (2020). The future of Arctic sea-ice biogeochemistry and ice-associated ecosystems. Nat. Clim. Chang. *10*, 983–992. https://doi.org/10.1038/s41558-020-00940-4.

42. Daase, M., Berge, J., Søreide, J.E., and Falk-Petersen, S. (2021). Ecology of arctic pelagic communities. In Arctic Ecology, D.N. Thomas, ed. (John Wiley & Sons), pp. 219–259. https://doi.org/10.1002/9781118846582.ch9.

43. Limoges, A., Weckström, K., Ribeiro, S., Georgiadis, E., Hansen, K.E., Martinez, P., Seidenkrantz, M.-S., Giraudeau, J., Crosta, X., and Massé, G. (2020). Learning from the past: Impact of the Arctic Oscillation on sea ice and marine productivity off northwest Greenland over the last 9,000 years. Glob. Chang. Biol. *26*, 6767–6786. https://doi.org/10.1111/gcb.15334.

44. Louis, M., Routledge, J., Heide-Jørgensen, M.P., Szpak, P., and Lorenzen, E.D. (2022). Sex and size matter: foraging ecology of offshore harbour porpoises in waters around Greenland. Mar. Biol. *169*, 140. https://doi.org/10.1007/s00227-022-04123-x.

45. Louis, M., Skovrind, M., Garde, E., Heide-Jørgensen, M.P., Szpak, P., and Lorenzen, E.D. (2021). Population-specific sex and size variation in long-term foraging ecology of belugas and narwhals. R. Soc. Open Sci. *8*, 202226. https://doi.org/10.1098/rsos.202226.

46. Sigman, D.M., and Casciotti, K.L. (2001). Nitrogen isotopes in the ocean. In Encyclopedia of Ocean Sciences, *3* (Academic Press), pp. 1884–1894.

47. Sherwood, O.A., Guilderson, T.P., Batista, F.C., Schiff, J.T., and McCarthy, M.D. (2014). Increasing subtropical North Pacific Ocean nitrogen fixation since the Little Ice Age. Nature *505*, 78–81. https://doi.org/10.1038/nature12784.

48. Baird, A.B., and Bickham, J.W. (2021). The stocks of bowheads. In The Bowhead Whale, J.C. George and J.G.M. Thewissen, eds. (Elsevier), pp. 19–29. https://doi.org/10.1016/B978-0-12-818969-6.00003-0.

49. Fortune, S.M.E., Young, B.G., and Ferguson, S.H. (2020). Age- and sex-specific movement, behaviour and habitat-use patterns of bowhead whales (Balaena mysticetus) in the Eastern Canadian Arctic. Polar Biol. *43*, 1725–1744. https://doi.org/10.1007/s00300-020-02739-7.

50. Pomerleau, C., Patterson, T.A., Luque, S., Lesage, V., Heide-Jørgensen, M.P., Dueck, L.L., and Ferguson, S.H. (2011). Bowhead whale Balaena mysticetus diving and movement patterns in the eastern Canadian Arctic: implications for foraging ecology. Endang. Species Res. *15*, 167–177. https://doi.org/10.3354/esr00373.

51. Kovacs, K.M., Lydersen, C., Vacquiè-Garcia, J., Shpak, O., Glazov, D., and Heide-Jørgensen, M.P. (2020). The endangered Spitsbergen bowhead whales' secrets revealed after hundreds of years in hiding. Biol. Lett. *16*, 20200148. https://doi.org/10.1098/rsbl.2020.0148.

52. Bertorelle, G., Raffini, F., Bosse, M., Bortoluzzi, C., Iannucci, A., Trucchi, E., Morales, H.E., and van Oosterhout, C. (2022). Genetic load: genomic estimates and applications in non-model animals. Nat. Rev. Genet. *23*, 492–503. https://doi.org/10.1038/s41576-022-00448-x.

53. Heide-Jørgensen, M.P., Hansen, R.G., and Shpak, O.V. (2021). Distribution, migrations, and ecology of the Atlantic and the Okhotsk Sea PopulationsChapter 5. In The Bowhead Whale, J.C. George and J.G.M. Thewissen, eds. (Academic Press), pp. 57–75. https://doi.org/10.1016/B978-0-12-818969-6.00005-4.

54. Mazet, O., Rodríguez, W., Grusea, S., Boitard, S., and Chikhi, L. (2016). On the importance of being structured: instantaneous coalescence rates and human evolution–lessons for ancestral population size inference? Heredity (Edinb) *116*, 362–371. https://doi.org/10.1038/hdy.2015.104.

55. Femerling, G., van Oosterhout, C., Feng, S., Bristol, R.M., Zhang, G., Groombridge, J., P Gilbert, M.T., and Morales, H.E. (2023). Genetic load and adaptive potential of a recovered avian species that narrowly avoided extinction. Mol. Biol. Evol. *40*, msad256. https://doi.org/10.1093/molbev/msad256.

56. Jackson, H.A., Percival-Alwyn, L., Ryan, C., Albeshr, M.F., Venturi, L., Morales, H.E., Mathers, T.C., Cocker, J., Speak, S.A., Accinelli, G.G., et al. (2022). Genomic erosion in a demographically recovered bird species during conservation rescue. Conserv. Biol. *36*, e13918. https://doi.org/10.1111/cobi.13918.

57. Pinto, A.V., Hansson, B., Patramanis, I., Morales, H.E., and van Oosterhout, C. (2023). The impact of habitat loss and population fragmentation on genomic erosion. Conserv. Genet. *25*, 49–57. https://doi.org/10.1007/s10592-023-01548-9.

58. Hansson, B., and Westerberg, L. (2002). On the correlation between heterozygosity and fitness in natural populations. Mol. Ecol. *11*, 2467–2474. https://doi.org/10.1046/j.1365-294X.2002.01644.x.

59. Harrisson, K.A., Pavlova, A., Telonis-Scott, M., and Sunnucks, P. (2014). Using genomics to characterize evolutionary potential for conservation of wild populations. Evol. Appl. *7*, 1008–1025. https://doi.org/10.1111/eva.12149.

60. Silver, L.W., Farquharson, K.A., Peel, E., Gilbert, M.T.P., Belov, K., Morales, H.E., and Hogg, C.J. (2025). Temporal loss of genome-wide and immunogenetic diversity in a near-extinct parrot. Mol. Ecol. *34*, e17746. https://doi.org/10.1111/mec.17746.

61. Chambault, P., Kovacs, K.M., Lydersen, C., Shpak, O., Teilmann, J., Albertsen, C.M., and Heide-Jørgensen, M.P. (2022). Future seasonal changes in habitat for Arctic whales during predicted ocean warming. Sci. Adv. *8*, eabn2422. https://doi.org/10.1126/sciadv.abn2422.

62. Freymueller, N.A., Lorenzen, E.D., Brown, S., Rahbek, C., and Fordham, D. (2025). 21st century sea ice loss will upend 11,700 years of suitable habitat for bowhead whales. Ecology & Evolution. https://doi.org/10.22541/au.173822517.74634727/v1.

63. de Jong, C. (1983). The Hunt of the Greenland Whale: A Short History and Statistical Sources (International Whaling Commission).

64. Rantanen, M., Karpechko, A.Y., Lipponen, A., Nordling, K., Hyvärinen, O., Ruosteenoja, K., Vihma, T., and Laaksonen, A. (2022). The Arctic has warmed nearly four times faster than the globe since 1979. Commun. Earth Environ. *3*, 1–10. https://doi.org/10.1038/s43247-022-00498-3.

65. Fordham, D.A., Jackson, S.T., Brown, S.C., Huntley, B., Brook, B.W., Dahl-Jensen, D., Gilbert, M.T.P., Otto-Bliesner, B.L., Svensson, A., Theodoridis, S., et al. (2020). Using paleo-archives to safeguard biodiversity under climate change. Science *369*, eabc5654. https://doi.org/10.1126/science.abc5654.

66. Sluijs, A., Schouten, S., Pagani, M., Woltering, M., Brinkhuis, H., Sinninghe Damsté, J.S., Dickens, G.R., Huber, M., Reichart, G.-J., Stein, R., et al. (2006). Subtropical Arctic Ocean temperatures during the Palaeocene/Eocene thermal maximum. Nature *441*, 610–613. https://doi.org/10.1038/nature04668.

67. Brown, S.C., Mellin, C., García Molinos, J., Lorenzen, E.D., and Fordham, D.A. (2022). Faster ocean warming threatens richest areas of marine biodiversity. Glob. Chang. Biol. *28*, 5849–5858. https://doi.org/10.1111/gcb.16328.

68. Moore, S.E. (2008). Marine Mammals as Ecosystem Sentinels. J. Mammal. *89*, 534–540. https://doi.org/10.1644/07-MAMM-S-312R1.1.

69. Stuiver, M., and Reimer, P.J. (1993). Extended ^{14}C data base and revised CALIB 3.0 ^{14}C age calibration program. Radiocarbon *35*, 215–230. https://doi.org/10.1017/S0033822200013904.

70. Hammer, Ø., Harper, D.A.T., and Ryan, P.D. (2001). PAST: Paleontological statistics software package for education and data analysis. Palaeontol. Electron. *4*, 9.

71. Blonder, B., and Harris, D.J. (2018). hypervolume: High dimensional geometry and set operations using kernel density estimation, support vector machines, and convex hulls. R package version 2. https://cran.r-project.org/web/packages/hypervolume/index.html.

72. R Core Team (2013). R: A Language and Environment for Statistical Computing (R Foundation for Statistical Computing).

73. Jiang, H., Lei, R., Ding, S.-W., and Zhu, S. (2014). Skewer: a fast and accurate adapter trimmer for next-generation sequencing paired-end reads. BMC Bioinformatics *15*, 182. https://doi.org/10.1186/1471-2105-15-182.

74. Chen, S., Zhou, Y., Chen, Y., and Gu, J. (2018). fastp: an ultra-fast all-in-one FASTQ preprocessor. Bioinformatics *34*, i884–i890. https://doi.org/10.1093/bioinformatics/bty560.

75. Li, H., and Durbin, R. (2009). Fast and accurate short read alignment with Burrows–Wheeler transform. Bioinformatics *25*, 1754–1760. https://doi.org/10.1093/bioinformatics/btp324.

76. Li, H., Handsaker, B., Wysoker, A., Fennell, T., Ruan, J., Homer, N., Marth, G., Abecasis, G., and Durbin, R.; 1000 Genome Project Data Processing Subgroup (2009). The Sequence Alignment/Map format and SAMtools. Bioinformatics *25*, 2078–2079. https://doi.org/10.1093/bioinformatics/btp352.

77. Jónsson, H., Ginolhac, A., Schubert, M., Johnson, P.L.F., and Orlando, L. (2013). mapDamage2.0: fast approximate Bayesian estimates of ancient DNA damage parameters. Bioinformatics *29*, 1682–1684. https://doi.org/10.1093/bioinformatics/btt193.

78. Grabherr, M.G., Russell, P., Meyer, M., Mauceli, E., Alföldi, J., Di Palma, F., and Lindblad-Toh, K. (2010). Genome-wide synteny through highly sensitive sequence alignment: Satsuma. Bioinformatics *26*, 1145–1151. https://doi.org/10.1093/bioinformatics/btq102.

79. Korneliussen, T.S., Albrechtsen, A., and Nielsen, R. (2014). ANGSD: Analysis of Next Generation Sequencing Data. BMC Bioinformatics *15*, 356. https://doi.org/10.1186/s12859-014-0356-4.

80. Cabrera, A.A., Rey-Iglesia, A., Louis, M., Skovrind, M., Westbury, M.V., and Lorenzen, E.D. (2022). How low can you go? Introducing SeXY: sex identification from low-quantity sequencing data despite lacking assembled sex chromosomes. Ecol. Evol. *12*, e9185. https://doi.org/10.1002/ece3.9185.

81. Meisner, J., and Albrechtsen, A. (2018). Inferring Population Structure and Admixture Proportions in Low-Depth NGS Data. Genetics *210*, 719–731. https://doi.org/10.1534/genetics.118.301336.

82. Skotte, L., Korneliussen, T.S., and Albrechtsen, A. (2013). Estimating individual admixture proportions from next generation sequencing data. Genetics *195*, 693–702. https://doi.org/10.1534/genetics.113.154138.

83. Taron, U.H., Lell, M., Barlow, A., and Paijmans, J.L.A. (2018). Testing of Alignment Parameters for Ancient Samples: Evaluating and Optimizing Mapping Parameters for Ancient Samples Using the TAPAS Tool. Genes *9*, 157. https://doi.org/10.3390/genes9030157.

84. Cheng, J.Y., Stern, A.J., Racimo, F., and Nielsen, R. (2022). Detecting selection in multiple populations by modeling ancestral admixture components. Mol. Biol. Evol. *39*, msab294. https://doi.org/10.1093/molbev/msab294.

85. Rasmussen, M.S., Garcia-Erill, G., Korneliussen, T.S., Wiuf, C., and Albrechtsen, A. (2022). Estimation of site frequency spectra from low-coverage sequencing data using stochastic EM reduces overfitting, runtime, and memory usage. Genetics *222*, iyac148. https://doi.org/10.1093/genetics/iyac148.

86. Santiago, E., Novo, I., Pardiñas, A.F., Saura, M., Wang, J., and Caballero, A. (2020). Recent Demographic History Inferred by High-Resolution Analysis of Linkage Disequilibrium. Mol. Biol. Evol. *37*, 3642–3653. https://doi.org/10.1093/molbev/msaa169.

87. Baumdicker, F., Bisschop, G., Goldstein, D., Gower, G., Ragsdale, A.P., Tsambos, G., Zhu, S., Eldon, B., Ellerman, E.C., Galloway, J.G., et al. (2022). Efficient ancestry and mutation simulation with msprime 1.0. Genetics *220*, iyab229. https://doi.org/10.1093/genetics/iyab229.

88. Haller, B.C., and Messer, P.W. (2019). SLiM 3: Forward Genetic Simulations Beyond the Wright-Fisher Model. Mol. Biol. Evol. *36*, 632–637. https://doi.org/10.1093/molbev/msy228.

89. Rozas, J., Ferrer-Mata, A., Sánchez-Delbarrio, J.C., Guirao-Rico, S., Librado, P., Ramos-Onsins, S.E., and Sánchez-Gracia, A. (2017). DnaSP 6: DNA Sequence Polymorphism Analysis of Large Data Sets. Mol. Biol. Evol. *34*, 3299–3302. https://doi.org/10.1093/molbev/msx248.

90. Leigh, J.W., and Bryant, D. (2015). popart: full-feature software for haplotype network construction. Methods Ecol. Evol. *6*, 1110–1116. https://doi.org/10.1111/2041-210X.12410.

91. Excoffier, L., and Lischer, H.E.L. (2010). Arlequin suite ver 3.5: a new series of programs to perform population genetics analyses under Linux and Windows. Mol. Ecol. Resour. *10*, 564–567. https://doi.org/10.1111/j.1755-0998.2010.02847.x.

92. Lanfear, R., Frandsen, P.B., Wright, A.M., Senfeld, T., and Calcott, B. (2017). PartitionFinder 2: New Methods for Selecting Partitioned Models of Evolution for Molecular and Morphological Phylogenetic Analyses. Mol. Biol. Evol. *34*, 772–773. https://doi.org/10.1093/molbev/msw260.

93. Bouckaert, R., Heled, J., Kühnert, D., Vaughan, T., Wu, C.H., Xie, D., Suchard, M.A., Rambaut, A., and Drummond, A.J. (2014). BEAST 2: A Software Platform for Bayesian Evolutionary Analysis. PLoS Comput. Biol. *10*, e1003537. https://doi.org/10.1371/journal.pcbi.1003537.

94. Rambaut, A., Drummond, A.J., Xie, D., Baele, G., and Suchard, M.A. (2018). Posterior Summarization in Bayesian Phylogenetics Using Tracer 1.7. Syst. Biol. *67*, 901–904. https://doi.org/10.1093/sysbio/syy032.

95. Hedges, R.E.M., Clement, J.G., Thomas, C.D.L., and O'Connell, T.C. (2007). Collagen turnover in the adult femoral mid-shaft: modeled from anthropogenic radiocarbon tracer measurements. Am. J. Phys. Anthropol. *133*, 808–816. https://doi.org/10.1002/ajpa.20598.

96. Hoffmann, A.A., and Willi, Y. (2008). Detecting genetic responses to environmental change. Nat. Rev. Genet. *9*, 421–432. https://doi.org/10.1038/nrg2339.

97. Wiig, Ø., Bachmann, L., and Hufthammer, A.K. (2019). Late Pleistocene and Holocene occurrence of bowhead whales (Balaena mysticetus) along the coasts of Norway. Polar Biol. *42*, 645–656. https://doi.org/10.1007/s00300-019-02460-0.

98. Dyke, A.S., and England, J. (2003). Canada's Most Northerly Postglacial Bowhead Whales (Balaena mysticetus): Holocene Sea-Ice Conditions and Polynya Development. Arctic *56*, 14–20. https://doi.org/10.14430/arctic598.

99. Atkinson, N., and England, J. (2004). Postglacial emergence of Amund and Ellef Ringnes islands, Nunavut: implications for the northwest sector of the Innuitian Ice Sheet. Can. J. Earth Sci. *41*, 271–283. https://doi.org/10.1139/e03-095.

100. Bednarski, J. (1990). An Early Holocene Bowhead Whale (Balaena mysticetus) in Nansen Sound, Canadian Arctic Archipelago. Arctic *43*, 50–54. https://doi.org/10.14430/arctic1590.

101. Bennike, O. (1997). Quaternary vertebrates from Greenland: A review. Quat. Sci. Rev. *16*, 899–909. https://doi.org/10.1016/S0277-3791(97)00002-4.

102. Bennike, O. (2008). An early Holocene Greenland whale from Melville Bugt, Greenland. Quat. Res. *69*, 72–76. https://doi.org/10.1016/j.yqres.2007.10.004.

103. Blake, W., Jr. (1992). Holocene emergence at Cape Herschel, east-central Ellesmere Island, Arctic Canada: implications for ice sheet configuration. Can. J. Earth Sci. *29*, 1958–1980. https://doi.org/10.1139/e92-153.

104. Dyke, A.S., and Morris, T.F. (1990). Postglacial History of the Bowhead Whale and of Driftwood Penetration: Implications for Paleoclimate, Central Canadian Arctic (Geological Survey of Canada).

105. King, R.H. (1991). Paleolimnology of a polar oasis, Truelove Lowland, Devon Island, N.W.T., Canada. Hydrobiologia *214*, 317–325. https://doi.org/10.1007/BF00050966.

106. Knuth, E. (1983). The northernmost ruins of the globe. Folk. Dansk Ethnografisk Tidsskrift Kobenhavn*25* (Dansk etnografisk forening), pp. 5–21.

107. Maxwell, M.S. (1985). Prehistory of the Eastern Arctic (Academic Press).

108. Morrison, D. (1989). Radiocarbon Dating Thule Culture. Arct. Anthropol. *26*, 48–77.

109. Sharpe, D.R. (1992). Quaternary Geology of Wollaston Peninsula, Victoria Island, Northwest Territories (Natural Resources Canada). https://doi.org/10.4095/134059.

110. Young, R.B., and King, R.H. (1989). Sediment chemistry and diatom stratigraphy of two high arctic isolation lakes, Truelove Lowland, Devon Island, N.W.T., Canada. J. Paleolimnol. *2*, 207–225. https://doi.org/10.1007/BF00202047.

111. Naughton, D. (2003). Annotated Bibliography of Quaternary Vertebrates of Northern North America: With Radiocarbon Dates (University of Toronto Press).

112. Hodgson, D.A. (1993). Surficial Geology, Storkerson Peninsula, Victoria Island and Stefansson Island, Northwest Territories. Map A 1817 (Geological Survey of Canada).

113. Dyke, A.S., and Savelle, J.M. (2003). Surficial Geology, Southern Prince Albert Sound, Victoria Island, Northwest Territories (NTS 87E/4, 87E/5). Open File 4321, scale 1:50 000 (Geological Survey of Canada).

114. Savelle, J.M., Dyke, A.S., Whitridge, P.J., and Poupart, M. (2012). Paleoeskimo Demography on Western Victoria Island, Arctic Canada: Implications for Social Organization and Longhouse Development. Arctic *65*, 167–181. https://doi.org/10.14430/arctic4198.

115. Dyke, A.S., and Savelle, J.M. (2004). Surficial Geology, Holman Area, Victoria Island, Northwest Territories (NTS 87F/10, 14, 15). Open File 4352, scale 1:50 000 (Geological Survey of Canada).

116. Dyke, A.S., and Savelle, J.M. (2006). Surficial Geology, Koch Island, Nunavut. Open File 4955, scale 1:50 000 (Geological Survey of Canada).

117. Dyke, A.S., and Savelle, J.M. (2000). Surficial Geology of the Lady Richardson Bay Area, Victoria Island, Nunavut and Northwest Territories (NTS 87C/8, 87C/9, 87C/10). Open File 3900, scale 1:50 000 (Geological Survey of Canada).

118. Dyke, A.S., and Savelle, J.M. (2002). Surficial Geology, Innirit Hills, Victoria Island, Nunavut (NTS 87D/4). Open File 3756, scale 1:50 000 (Geological Survey of Canada).

119. Dyke, A.S., and Savelle, J.M. (2004). Surficial Geology, Page Point Area, Victoria Island, Northwest Territories (NTS 87E/10, 15). Open File 4336, scale 1:50 000 (Geological Survey of Canada).

120. Savelle, J.M., Dyke, A.S., and Poupart, M. (2009). Paleo-Eskimo Occupation History of Foxe Basin, Nunavut: Implications for the "Core Area". In The Northern World, AD 900-1400, H. Maschner, O. Mason, and R. McGhee, eds. (The University of Utah Press), pp. 209–234.

121. Dyke, A.S., and Savelle, J.M. (2009). Paleoeskimo Demography and Sea-Level History, Kent Peninsula and King William Island, Central Northwest Passage, Arctic Canada. Arctic *62*, 371–392. https://doi.org/10.14430/arctic169.

122. Dyke, A.S., Savelle, J.M., and Johnson, D.S. (2011). Paleoeskimo Demography and Holocene Sea-level History, Gulf of Boothia, Arctic Canada. Arctic *64*, 151–168. https://doi.org/10.14430/arctic4096.

123. Savelle, J.M., and Dyke, A.S. (2014). Paleoeskimo Occupation History of Foxe Basin, Arctic Canada: Implications for the Core Area Model and Dorset Origins. Am. Antiq. *79*, 249–276. https://doi.org/10.7183/0002-7316.79.2.249.

124. Dyke, A.S., and Savelle, J.M. (2001). Holocene History of the Bering Sea Bowhead Whale (Balaena Mysticetus) in Its Beaufort Sea Summer Grounds off Southwestern Victoria Island, Western Canadian Arctic1. Quat. Res. *55*, 371–379. https://doi.org/10.1006/qres.2001.2228.

125. Salvigsen, O., Elgersma, A., and Landvik, J.Y. (1991). Radiocarbon dated raised beaches in northwestern Wedel Jarlsberg land, Spitsbergen, Svalbard. In Wyprawy Geograficzne na Spitsbergen (Maria Curie-Skłodowska University), pp. 9–16.

126. Salvigsen, O., and Elgersma, A. (1993). Radiocarbon dating of deglaciation and raised beaches in north-western Sorkapp Land, Spitsbergen, Svalbard. Zeszyty Naukowe Uniwersytetu *94*, 39–48.

127. Salvigsen, O., Elgersma, A., Hjort, C., Lagerlund, E., Liestøl, O., and Svensson, N.-O. (1990). Glacial history and shoreline displacement on Erdmannflya and Bohemanflya, Spitsbergen, Svalbard. Polar Res. *8*, 261–273.

128. Salvigsen, O. (1977). Radiocarbon datings and the extension of the Weichselian ice-sheet in Svalbard. Norsk Polarinstitutt Årbok *1976*, 209–224.

129. Landvik, J.Y., Hansen, A., Kelly, M., and Salvigsen, O. (1992). The last deglaciation and glacimarine/marine sedimentation on Barentsøya and Edgeøya, eastern Svalbard. Oceanogr. Lit. Rev. *40*, 998.

130. Jensen, A.M. (2009). Radiocarbon dates from recent excavations at Nuvuk, Point Barrow, Alaska and their implications for Neoeskimo prehistory. In On the track of the Thule Culture from Bering Strait to East Greenland. Proceedings of the SILA Conference "The Thule Culture—New Perspectives in Inuit Prehistory" (National Museum Studies in Archaeology & History), pp. 45–62.

131. Park, R.W. (1989). Porden Point: An Intrasite Approach to Settlement System Analysis. PhD thesis (Department of Anthropology, University of Alberta).

132. Stuart, A.J., and Lister, A.M. (2012). Extinction chronology of the woolly rhinoceros Coelodonta antiquitatis in the context of late Quaternary megafaunal extinctions in northern Eurasia. Quat. Sci. Rev. *51*, 1–17. https://doi.org/10.1016/j.quascirev.2012.06.007.

133. Stafford, T.W., Jull, A.J.T., Brendel, K., Duhamel, R.C., and Donahue, D. (1987). Study of Bone Radiocarbon Dating Accuracy at the University of Arizona NSF Accelerator Facility for Radioisotope Analysis. Radiocarbon *29*, 24–44. https://doi.org/10.1017/S0033822200043538.

134. Talamo, S., Fewlass, H., Maria, R., and Jaouen, K. (2021). "Here we go again": the inspection of collagen extraction protocols for 14C dating and palaeodietary analysis. Sci. Technol. Archaeol. Res. *7*, 62–77. https://doi.org/10.1080/20548923.2021.1944479.

135. Furze, M.F.A., Pieńkowski, A.J., and Coulthard, R.D. (2014). New cetacean ΔR values for Arctic North America and their implications for marine-mammal-based palaeoenvironmental reconstructions. Quat. Sci. Rev. *91*, 218–241. https://doi.org/10.1016/j.quascirev.2013.08.021.

136. Jensen, A.M. (2009). Nuvuk: Point Barrow, Alaska: the Thule cemetery and Ipiutak occupation. PhD thesis (Bryn Mawr College).

137. Mangerud, J., Bondevik, S., Gulliksen, S., Karin Hufthammer, A., and Høisæter, T. (2006). Marine 14C reservoir ages for 19th century whales and molluscs from the North Atlantic. Quat. Sci. Rev. *25*, 3228–3245. https://doi.org/10.1016/j.quascirev.2006.03.010.

138. Armstrong, E., Hopcroft, P.O., and Valdes, P.J. (2019). A simulated Northern Hemisphere terrestrial climate dataset for the past 60,000 years. Sci. Data *6*, 265. https://doi.org/10.1038/s41597-019-0277-1.

139. Dansgaard, W., Johnsen, S.J., Clausen, H.B., Dahl-Jensen, D., Gundestrup, N.S., Hammer, C.U., Hvidberg, C.S., Steffensen, J.P., Sveinbjörnsdottir, A.E., Jouzel, J., et al. (1993). Evidence for general instability of past climate from a 250-kyr ice-core record. Nature *364*, 218–220. https://doi.org/10.1038/364218a0.

140. Heinrich, H. (1988). Origin and Consequences of Cyclic Ice Rafting in the Northeast Atlantic Ocean During the Past 130,000 Years. Quat. Res. *29*, 142–152. https://doi.org/10.1016/0033-5894(88)90057-9.

141. Gregory, J.M., Stott, P.A., Cresswell, D.J., Rayner, N.A., Gordon, C., and Sexton, D.M.H. (2002). Recent and future changes in Arctic sea ice simulated by the HadCM3 AOGCM. Geophys. Res. Lett. *29*. 28-1–28. https://doi.org/10.1029/2001GL014575.

142. Beyer, R., Krapp, M., and Manica, A. (2020). An empirical evaluation of bias correction methods for palaeoclimate simulations. Clim. Past *16*, 1493–1508. https://doi.org/10.5194/cp-16-1493-2020.

143. Fordham, D.A., Saltré, F., Haythorne, S., Wigley, T.M.L., Otto-Bliesner, B.L., Chan, K.C., and Brook, B.W. (2017). PaleoView: a tool for generating continuous climate projections spanning the last 21 000 years at regional and global scales. Ecography *40*, 1348–1358. https://doi.org/10.1111/ecog.03031.

144. Compo, G.P., Whitaker, J.S., Sardeshmukh, P.D., Matsui, N., Allan, R.J., Yin, X., Gleason, B.E., Vose, R.S., Rutledge, G., Bessemoulin, P., et al. (2011). The twentieth century reanalysis project. Q. J. R. Meteorol. Soc. *137*, 1–28. https://doi.org/10.1002/qj.776.

145. Austin, M.P. (2002). Spatial prediction of species distribution: an interface between ecological theory and statistical modelling. Ecol. Modell. *157*, 101–118. https://doi.org/10.1016/S0304-3800(02)00205-3.

146. Nogués-Bravo, D. (2009). Predicting the past distribution of species climatic niches. Glob. Ecol. Biogeogr. *18*, 521–531. https://doi.org/10.1111/j.1466-8238.2009.00476.x.

147. Elith, J., and Leathwick, J.R. (2009). Species distribution models: Ecological explanation and prediction across space and time. Annu. Rev. Ecol. Evol. Syst. *40*, 677–697. https://doi.org/10.1146/annurev.ecolsys.110308.120159.

148. Bluhm, B.A., and Gradinger, R. (2008). Regional variability in food availability for Arctic marine mammals. Ecol. Appl. *18*, S77–S96. https://doi.org/10.1890/06-0562.1.

149. Hutchinson, G.E. (1957). Concluding remarks. Cold Spring Harb. Symp. Quant. Biol. *22*, 415–427. https://doi.org/10.1101/SQB.1957.022.01.039.

150. Blonder, B., Morrow, C.B., Maitner, B., Harris, D.J., Lamanna, C., Violle, C., Enquist, B.J., and Kerkhoff, A.J. (2018). New approaches for delineating n -dimensional hypervolumes. Methods Ecol. Evol. *9*, 305–319. https://doi.org/10.1111/2041-210X.12865.

151. Fordham, D.A., Brown, S.C., Akçakaya, H.R., Brook, B.W., Haythorne, S., Manica, A., Shoemaker, K.T., Austin, J.J., Blonder, B., Pilowsky, J.A., et al. (2022). Process-explicit models reveal pathway to extinction for woolly mammoth using pattern-oriented validation. Ecol. Lett. *25*, 125–137. https://doi.org/10.1111/ele.13911.

152. Phillips, S.J., Anderson, R.P., and Schapire, R.E. (2006). Maximum entropy modeling of species geographic distributions. Ecol. Modell. *190*, 231–259. https://doi.org/10.1016/j.ecolmodel.2005.03.026.

153. Belikov, S.E., Gorbunov, Y.A., and Shil'nikov, V.I. (1989). Distribution of pinnipedia and cetacea in Soviet Arctic seas and the Bering Sea in winter. Sov. J. Mar. Biol. *15*, 251–257.

154. Petrov, S.A., Isachenko, A.I., Glebova, M.A., Gavrilov, Y.G.,F.S.A., Ponomartsev, N.V., Semenov, A.G., Kuchin, S.O., Shishman, C.M., and Pavlov, V.A. (2018). The results of marine mammal countins during the four expeditions in the Arctic in 2014 and 2015. In 9th International Conference on "Marine Mammals of Holarctic", pp. 91–102.

155. Gavrilo, M.V., and Tretiakov, V.Y. (2008). Observation of bowhead whales (*Balaena mysticetus*) in the East-Siberian Sea during 2007 season with record-low ice cover. In The 5th International Conference on "Marine Mammals of Holarctic", pp. 191–193.

156. Boyce, M.S., Vernier, P.R., Nielsen, S.E., and Schmiegelow, F.K.A. (2002). Evaluating resource selection functions. Ecol. Modell. *157*, 281–300. https://doi.org/10.1016/S0304-3800(02)00200-4.

157. Hirzel, A.H., Le Lay, G., Helfer, V., Randin, C., and Guisan, A. (2006). Evaluating the ability of habitat suitability models to predict species presences. Ecol. Modell. *199*, 142–152. https://doi.org/10.1016/j.ecolmodel.2006.05.017.

158. Qi, H., Coplen, T.B., Geilmann, H., Brand, W.A., and Böhlke, J.K. (2003). Two new organic reference materials for δ13C and δ15N measurements and a new value for the δ13C of NBS 22 oil. Rapid Commun. Mass Spectrom. *17*, 2483–2487. https://doi.org/10.1002/rcm.1219.

159. Qi, H., Coplen, T.B., Mroczkowski, S.J., Brand, W.A., Brandes, L., Geilmann, H., and Schimmelmann, A. (2016). A new organic reference material, l-glutamic acid, USGS41a, for $\delta^{13}C$ and $\delta^{15}N$ measurements – a replacement for USGS41. Rapid Commun. Mass Spectrom. *30*, 859–866. https://doi.org/10.1002/rcm.7510.

160. Szpak, P., Metcalfe, J.Z., and Macdonald, R.A. (2017). Best practices for calibrating and reporting stable isotope measurements in archaeology. J. Archaeol. Sci. Rep. *13*, 609–616. https://doi.org/10.1016/j.jasrep.2017.05.007.

161. Dabney, J., Knapp, M., Glocke, I., Gansauge, M.-T., Weihmann, A., Nickel, B., Valdiosera, C., García, N., Pääbo, S., Arsuaga, J.-L., et al. (2013). Complete mitochondrial genome sequence of a Middle Pleistocene cave bear reconstructed from ultrashort DNA fragments. Proc. Natl. Acad. Sci. USA *110*, 15758–15763. https://doi.org/10.1073/pnas.1314445110.

162. Allentoft, M.E., Sikora, M., Sjögren, K.-G., Rasmussen, S., Rasmussen, M., Stenderup, J., Damgaard, P.B., Schroeder, H., Ahlström, T., Vinner, L., et al. (2015). Population genomics of Bronze Age Eurasia. Nature *522*, 167–172. https://doi.org/10.1038/nature14507.

163. Briggs, A.W., Stenzel, U., Meyer, M., Krause, J., Kircher, M., and Pääbo, S. (2010). Removal of deaminated cytosines and detection of in vivo methylation in ancient DNA. Nucleic Acids Res. *38*, e87. https://doi.org/10.1093/nar/gkp1163.

164. Carøe, C., Gopalakrishnan, S., Vinner, L., Mak, S.S.T., Sinding, M.H.S., Samaniego, J.A., Wales, N., Sicheritz-Pontén, T., and Gilbert, M.T.P. (2018). Single-tube library preparation for degraded DNA. Methods Ecol. Evol. *9*, 410–419. https://doi.org/10.1111/2041-210X.12871.

165. Keane, M., Semeiks, J., Webb, A.E., Li, Y.I., Quesada, V., Craig, T., Madsen, L.B., van Dam, S., Brawand, D., Marques, P.I., et al. (2015). Insights into the evolution of longevity from the bowhead whale genome. Cell Rep. *10*, 112–122. https://doi.org/10.1016/j.celrep.2014.12.008.

166. Nyhus, E.S., Lindqvist, C., Kovacs, K., Lydersen, C., Wiig, Ø., and Bachmann, L. (2016). Mitogenomes of contemporary Spitsbergen stock bowhead whales (Balaena mysticetus). Mitochondrial DNA B Resour. *1*, 898–900. https://doi.org/10.1080/23802359.2016.1258345.

167. Hanghøj, K., Moltke, I., Andersen, P.A., Manica, A., and Korneliussen, T.S. (2019). Fast and accurate relatedness estimation from high-throughput sequencing data in the presence of inbreeding. GigaScience *8*, giz034. https://doi.org/10.1093/gigascience/giz034.

168. Patterson, N., Price, A.L., and Reich, D. (2006). Population structure and eigenanalysis. PLoS Genet. *2*, e190. https://doi.org/10.1371/journal.pgen.0020190.

169. Wang, L., Zhang, W., and Li, Q. (2020). AssocTests: An R package for genetic association studies. J. Stat. Softw. *94*, 1–26. https://doi.org/10.18637/jss.v094.i05.

170. Hui, R., D'Atanasio, E., Cassidy, L.M., Scheib, C.L., and Kivisild, T. (2020). Evaluating genotype imputation pipeline for ultra-low coverage ancient genomes. Sci. Rep. *10*, 18542. https://doi.org/10.1038/s41598-020-75387-w.

171. Beaumont, M.A., Zhang, W., and Balding, D.J. (2002). Approximate Bayesian computation in population genetics. Genetics *162*, 2025–2035. https://doi.org/10.1093/genetics/162.4.2025.

172. Frankham, R. (2007). Effective population size/adult population size ratios in wildlife: a review. Genet. Res. *89*, 491–503. https://doi.org/10.1017/S0016672308009695.

173. Givens, G.H., Edmondson, S.L., George, J.C., Suydam, R., Charif, R.A., Rahaman, A., Hawthorne, D., Tudor, B., DeLong, R.A., and Clark, C.W. (2016). Horvitz–Thompson whale abundance estimation adjusting for uncertain recapture, temporal availability variation, and intermittent effort. Environmetrics *27*, 134–146. https://doi.org/10.1002/env.2379.

174. Ferguson, S.H., Higdon, J.W., Hall, P.A., Hansen, R.G., and Doniol-Valcroze, T. (2021). Developing a precautionary management approach for the Eastern Canada-West Greenland population of bowhead whales (Balaena mysticetus). Front. Mar. Sci. *8*. https://doi.org/10.3389/fmars.2021.709989.

175. Kardos, M., Armstrong, E.E., Fitzpatrick, S.W., Hauser, S., Hedrick, P.W., Miller, J.M., Tallmon, D.A., and Funk, W.C. (2021). The crucial role of genome-wide genetic variation in conservation. Proc. Natl. Acad. Sci. USA *118*, e2104642118. https://doi.org/10.1073/pnas.2104642118.

176. Yim, H.-S., Cho, Y.S., Guang, X., Kang, S.G., Jeong, J.-Y., Cha, S.-S., Oh, H.-M., Lee, J.-H., Yang, E.C., Kwon, K.K., et al. (2014). Minke whale genome and aquatic adaptation in cetaceans. Nat. Genet. *46*, 88–92. https://doi.org/10.1038/ng.2835.

177. Ralls, K., Ballou, J.D., and Templeton, A. (1988). Estimates of lethal equivalents and the cost of inbreeding in mammals. Conserv. Biol. *2*, 185–193. https://doi.org/10.1111/j.1523-1739.1988.tb00169.x.

178. Self, S.G., and Liang, K.-Y. (1987). Asymptotic Properties of Maximum Likelihood Estimators and Likelihood Ratio Tests under Nonstandard Conditions. J. Am. Stat. Assoc. *82*, 605–610. https://doi.org/10.1080/01621459.1987.10478472.

179. Kelleher, J., Thornton, K.R., Ashander, J., and Ralph, P.L. (2018). Efficient pedigree recording for fast population genetics simulation. PLoS Comput. Biol. *14*, e1006581. https://doi.org/10.1371/journal.pcbi.1006581.

180. Kelleher, J., and Lohse, K. (2020). Coalescent Simulation with msprime. Methods Mol. Biol. *2090*, 191–230. https://doi.org/10.1007/978-1-0716-0199-0_9.

181. Kardos, M., Zhang, Y., Parsons, K.M., A, Y., Kang, H., Xu, X., Liu, X., Matkin, C.O., Zhang, P., Ward, E.J., et al. (2023). Inbreeding depression explains killer whale population dynamics. Nat. Ecol. Evol. *7*, 675–686. https://doi.org/10.1038/s41559-023-01995-0.

182. Liu, X., and Fu, Y.-X. (2015). Exploring population size changes using SNP frequency spectra. Nat. Genet. *47*, 555–559. https://doi.org/10.1038/ng.3254.

183. Excoffier, L., Marchi, N., Marques, D.A., Matthey-Doret, R., Gouy, A., and Sousa, V.C. (2021). Fastsimcoal2: Demographic inference under complex evolutionary scenarios. Bioinformatics *37*, 4882–4885. https://doi.org/10.1093/bioinformatics/btab468.

184. Nei, M. (1987). Molecular Evolutionary Genetics (Columbia University Press). https://doi.org/10.7312/nei-92038.

185. Bandelt, H.J., Macaulay, V., and Richards, M. (2000). Median networks: speedy construction and greedy reduction, one simulation, and two case studies from human mtDNA. Mol. Phylogenet. Evol. *16*, 8–28. https://doi.org/10.1006/mpev.2000.0792.

186. Drummond, A.J., Rambaut, A., Shapiro, B., and Pybus, O.G. (2005). Bayesian Coalescent Inference of Past Population Dynamics from Molecular Sequences. Mol. Biol. Evol. *22*, 1185–1192. https://doi.org/10.1093/molbev/msi103.

Please cite this article in press as: Westbury et al., Four centuries of commercial whaling eroded 11,000 years of population stability in bowhead whales, Cell (2026), https://doi.org/10.1016/j.cell.2026.02.022

STAR★METHODS

KEY RESOURCES TABLE

REAGENT or RESOURCE	SOURCE	IDENTIFIER
Deposited data		
Subfossil bowhead whale bones	This study	PRJNA1174153
Contemporary bowhead whale genomes (ECWG)	This study	PRJNA1174153
Contemporary bowhead whale genomes (EGSB)	NCBI	PRJNA643010
Bowhead whale mitochondrial genome	NCBI	KY026773.1
Bowhead whale nuclear reference genome	N/A	bowhead-whale.org
Cow X chromosome	NCBI	CM008168.2
Human Y chromosome	NCBI	NC_000024.10
Right whale genome	NCBI BioSample	SAMN32746534
Chemicals, peptides, and recombinant proteins		
Monarch® DNA Cleanup Columns (5 μg)	New England Biolabs	T1034L
Buffer PE (concentrate 100 ml)	Qiagen	19065
KAPA HiFi HotStart Uracil+ ReadyMix (2X)	Roche	KK2801/KK2802
Thermolabile USER® II Enzyme (250 U)	New England Biolabs	M5508L
T4 Polynucleotide Kinase	New England Biolabs	M0201L
T4 DNA Polymerase	New England Biolabs	M0203L
T4 DNA Ligase	New England Biolabs	M0202L
Bst 2.0 WarmStart DNA Polymerase	New England Biolabs	M0538L
PEG 4000 50%	Molecular Dimensions	MD2-100-11
UltraPure 1 M Tris-HCl pH 7.5	Sigma	15567027
Dimethyl sulfoxide (DMSO)	Sigma-Aldrich	D8418-50ML
SYBR Green	Invitrogen	S7563
ROX reference dye	Invitrogen	12223-012
Software and algorithms		
Calib v7.0.4	Stuiver and Reimer[69]	https://calib.org/calib/
PAST v4.03	Hammer et al.[70]	https://www.nhm.uio.no/english/research/resources/past/
Hypervolume (R package)	Blonder and Harris[71]	https://cran.r-project.org/web/packages/hypervolume/index.html
R v4.1.1	R Core Team[72]	https://www.r-project.org/
skewer v0.2.2	Jiang et al.[73]	https://github.com/relipmoc/skewer
fastp v0.20.1	Chen et al.[74]	https://github.com/OpenGene/fastp
BWA v0.7.15	Li and Durbin[75]	https://github.com/lh3/bwa
SAMtools v1.6	Li et al.[76]	https://github.com/samtools/samtools
mapDamage v2	Jónsson et al.[77]	https://github.com/ginolhac/mapDamage
satsuma synteny v2.1	Grabherr et al.[78]	https://github.com/bioinfologics/satsuma2
ANGSD v0.921 + realSFS	Korneliussen et al.[79]	http://www.popgen.dk/angsd/
SeXY	Cabrera et al.[80]	https://github.com/andreidae/SeXY
PCAngsd v0.95	Meisner and Albrechtsen[81]	https://github.com/Rosemeis/pcangsd
NGSadmix	Skotte et al.[82]	https://github.com/aalbrechtsen/NGSadmix
TAPAS v1.2	Taron et al.[83]	https://mlell.github.io/tapas/
popgenWindows.py (genomics_general)	N/A	https://github.com/simonhmartin/genomics_general

(*Continued on next page*)

Please cite this article in press as: Westbury et al., Four centuries of commercial whaling eroded 11,000 years of population stability in bowhead whales, Cell (2026), https://doi.org/10.1016/j.cell.2026.02.022

Continued

REAGENT or RESOURCE	SOURCE	IDENTIFIER
Ohana	Cheng et al.[84]	https://github.com/jade-cheng/ohana
SimGL	N/A	https://github.com/RacimoLab/simGL
winsfs v0.7	Rasmussen et al.[85]	https://github.com/malthesr/winsfs
GONE	Santiago et al.[86]	https://github.com/esrud/GONE
Msprime	Baumdicker et al.[87]	https://github.com/tskit-dev/msprime
SLiM 3	Haller and Messer[88]	https://messerlab.org/slim/
DnaSP v6.12.03	Rozas et al.[89]	http://www.ub.edu/dnasp/
PopART	Leigh and Bryant[90]	https://popart.maths.otago.ac.nz/
Arlequin v3.5	Excoffier and Lischer[91]	http://cmpg.unibe.ch/software/arlequin35/
PartitionFinder v2.1.1	Lanfear et al.[92]	https://github.com/brettc/partitionfinder
BEAST v2.6.1	Bouckaert et al.[93]	https://www.beast2.org/
Tracer v1.7.1	Rambaut et al.[94]	https://github.com/beast-dev/tracer

EXPERIMENTAL MODEL AND STUDY PARTICIPANT DETAILS

The foundation of this study is two time series of radiocarbon dated subfossil bowhead whales (*Balaena mysticetus*) spanning the Holocene (Figure 1A). The fossils – from the Canadian Arctic Archipelago and the Svalbard Archipelago (Norway) – were collected in the field and partly radiocarbon dated by geologists in the 1980s and 1990s. Based on their individual radiocarbon age and relative placement on raised beach ridges, the fossils were previously used to estimate Holocene changes of sea ice, sea level, and glaciation.[33,34]

In essence, the two time series represent geographically independent lenses into the Holocene history of bowhead whales, one from the western sector of the Atlantic Arctic (Canadian Arctic Archipelago), the other from the eastern sector of the Atlantic Arctic (Svalbard Archipelago). We revisited the two fossil chronologies, and analysed a subsample of the bowhead whale specimens using stable $\delta^{13}C$ and $\delta^{15}N$ isotopes and ancient DNA. This overlap in the fossil record allows us to draw comparisons between environmental changes and genetic changes, aligning different rates of response within a single temporal framework.

Bone collagen stable $\delta^{13}C$ and $\delta^{15}N$ isotope values provide data on the foraging ecology and feeding habitat of individuals, averaged over years to decades.[95] Thus, the temporal resolution of these data are on the time span of the past years to decades, relative to the age of the specimen. Thus in the context of the 11,000 years investigated in our study, the stable isotope data provide insights into shorter-term ecological and food-web changes, reflecting shifts in feeding habitat and prey composition that respond relatively quickly to climate fluctuations.

The genetic profiles of the fossil specimens were compared with contemporary bowhead whale individuals from each area (Figure 1A), to investigate spatiotemporal patterns of substructuring and diversity across the Atlantic Arctic. Genetic data capture changes over more extended periods, reflecting population-level responses to longer-term environmental pressures, which are often cumulative and only detectable after multiple generations.[96] However, because our palaeogenomic data come from a chronological series of fossils spanning thousands of years, we are able to track gradual genetic changes alongside the shorter-term ecological shifts revealed by isotopic data. To take our genetic results into the future, we incorporated forward-in-time genomic/evolutionary simulations to assess the long-term impacts of commercial whaling derived from our results comparing the fossil and contemporary individuals.

We used the global fossil chronology of bowhead whales, comprising 823 radiocarbon dated fossils (140 of which are from this study) and reconstructions of climate and environmental conditions to inform ecological models and estimate bowhead whale habitat suitability at fine spatial and temporal resolutions throughout the Holocene. Our modelling approach provides broad-scale insights into how the geographic distribution of suitable habitat for bowhead whales shifted in response to climate-driven environmental change at generational timescales. The fine temporal resolution of our spatial analysis delivers information on species–environment relationships that are scalable to current-day conservation management and policy decisions.[65] When integrated with genetic and isotopic datasets, these ecological models enable us to link population-level responses inferred from DNA to the dynamics and distribution of habitat availability, offering a more holistic view of how past environmental change has shaped bowhead whale ecology and evolution.

Bowhead samples

All specimens analysed from the Canadian Arctic Archipelago were previously identified in the field as bowhead whales. The specimens from the Svalbard Archipelago were identified from ancient DNA.[29] For ecological modelling, we compiled a record of previously unreported and already available radiocarbon dated subfossil bowhead whales from across the circumpolar Arctic, totalling 823 individuals after filtering[29,33,97–131] (Table S2). To ensure the reliability of our radiocarbon dates, we implemented an auditing

criteria guided by the criteria described in Stuart and Lister.[132] We included only fossils that were known to be from bowhead whales and that had been dated using AMS radiocarbon dating. As a further precaution, we excluded samples processed before 1980 CE if we did not have information on whether dating of the specimen was performed using AMS radiocarbon dating on collagen and with adequate pretreatment (especially cleaning), as these protocols were not in regular use until the early 1980s.[132,133] Radiocarbon dates used in this study were produced at multiple laboratories using standard pretreatment methods appropriate to the time and material type. For many historical or externally sourced dates, individual-level pretreatment data were not retrievable. While ultrafiltration is often applied to reduce contamination, it is not without limitations and may itself introduce modern or fossil carbon if filters are insufficiently cleaned.[134] Therefore, we did not require this as a strict filtering criteria.

The largest number of specimens suitable for ecological modelling were from the Canadian Arctic Archipelago and Svalbard Archipelago chronologies; a subset of these samples were analysed using ancient biomolecules, mentioned above and detailed later. We included 60 previously unreported radiocarbon dates of bowhead fossils from around the Svalbard Archipelago, and East Greenland (Table S2). The samples were identified and dated following.[97] We also included 80 previously unreported radiocarbon dates from bowhead whale fossils from around the Central Canadian Archipelago, which were identified and dated following.[33] This yielded a total of 823 fossils with reliable radiocarbon dates.

To ensure comparability between sample ages across our analyses, we recalibrated all original radiocarbon dates with Calib v7.0.4 [69] using the marine13 calibration curve, a specified age span of 100 years, and unique marine reservoir correction (delta R) values depending on the region in which the specimen was found. For samples from the Canadian Arctic (n = 652) we used a delta R of 170±95[135]; from around Alaska (n = 4), we used a delta R of 506±83[136]; from the Svalbard Archipelago and the Norwegian coast (n = 167), we used a delta R of 7±39.[137] Due to the marine reservoir effect complicating the calibration of individuals dated to within the last ~500 years, individuals that produced nonsensical ages (e.g. negative results) were given an age of 500 years BP.

For stable isotope and ancient DNA analyses, we sub-sampled radiocarbon dated bowhead whale bone specimens from the Canadian Museum of Nature, Ottawa (Canadian Arctic Archipelago samples) and the Natural History Museum, University of Oslo (Svalbard Archipelago samples). All except one Canadian sample (>33 kya) and three Late Pleistocene Svalbard samples were dated to, or close to, the Holocene. An overview of the samples and their associated biomolecular data is included in Tables S3 (stable δ^{13}C and δ^{15}N isotopes) and S4 (ancient DNA).

Contemporary bowhead whales are recognised as belonging to four distinct management units (termed stocks or breeding populations), based on genetics and non-genetic data (incl. telemetry).[48] To contextualise the Holocene ancient DNA data, we included comparable genomic data from samples collected from the two contemporary stocks in the Atlantic Arctic. We generated genomic data from seven samples from the contemporary 'East Canada-West Greenland' stock, and downloaded published genomic data from 12 bowhead individuals from the 'East Greenland-Svalbard-Barents Sea' stock (sampled 2017-2018, Genbank bioproject: PRJNA643010).[22] Sample and data overviews for the contemporary samples are provided in Extended data table 6.

METHOD DETAILS

Ecological niche modelling

Climate data

Palaeoclimate data were accessed using a high resolution (1° x 1°) oceanic climate dataset for the period 60 thousand years ago (kya) through to the present (1950 CE).[138] These data were generated by temporally linking discrete snapshot simulations from the HadCM3B-M2.1 coupled general circulation model.[35] The HadCM3B-M2.1 model has a nominal oceanic resolution of 1.25° × 1.25° and is run as a series of snapshots at 1,000-year intervals between 0 (1950 CE) and 22 kya, and 2,000-year intervals between 60 kya and 22 kya. The snapshot simulations have been linked using splines based on monthly climatologies, before interannual and millennial scale variability (e.g. Dansgaard-Oeschger[139] and Heinrich[140] events) was imposed on the timeseries. The data has been downscaled to the final 1° × 1° resolution using bilinear interpolation. Tests of the HadCM3B-M2.1 model show that it reproduces global and regional sea-surface temperatures and surface salinity.[35] While no validation of the HadCM3B-M2.1 sea-ice dynamics has been done, a validation using the same underlying model (HadCM3), has shown a good fit to observed sea-ice extents and declines.[141]

Simulation of the climate system by even the most advanced global climate models contain notable biases.[142] Consequently, it is crucial to address these model biases in order to achieve realistic palaeoclimate simulations for use in studies of long-term ecological dynamics.[143] Our climate data were bias-corrected using an additive delta (change-factor) method[142] for sea surface temperature, and a multiplicative correction for sea surface salinity and sea ice concentration (sea ice cover). Sea surface temperature and salinity were bias corrected against the World Ocean Atlas 2018 dataset (https://www.ncei.noaa.gov/products/world-ocean-atlas), with sea ice cover corrected against the Twentieth Century Reanalysis dataset[144] using a climatological period of 1850-1950 CE. Multiplicative bias corrections were capped at 3x the simulated value.[138] Corrected sea ice cover values that exceeded 100% were truncated back to 100%. No bias-correction was done on sea ice thickness due to there not being a suitable dataset covering the end of the model simulation period (1850-1950 CE).

The resulting palaeoclimate simulations were a continuous time series of maps of climatological monthly averages, calculated over a 30-yr window, with a step of 50 years, for the period 60 kya to 0 kya. We extracted seasonal data for sea surface temperature (SST; °C), sea surface salinity (SAL, ‰), sea ice cover (SIC, % of the study area covered by sea ice), and sea ice thickness (SIT, m) for our

Please cite this article in press as: Westbury et al., Four centuries of commercial whaling eroded 11,000 years of population stability in bowhead whales, Cell (2026), https://doi.org/10.1016/j.cell.2026.02.022

study region. This data was then used to generate 30-yr averages of four variables (for each season) at 50-year timesteps: (i) seasonal mean SST; (ii) seasonal mean SAL; (iii) seasonal mean SIC; and (iv) seasonal mean SIT. All fossil records for bowhead whales were then matched to this data and used to calibrate an ecological niche model.

Following exploratory data analyses we opted to use summer (June, July, August) SST, SAL, SIC in our ecological niche model. We did not use summer SIT as we were unable to bias-correct it. These metrics are theorised to be as successful as more direct (proximal) variables in predicting the relationships between environmental pattern and process, particularly in extreme environments where species are not occupying optimal parts of their potential realised niches.[145–147] The choice of summer seasonal data is justified as we have a large number of samples above the northern edge of the contemporary Canadian Arctic Archipelago population boundary (Figure 1), and bowhead whales from this region are known to move northwards in summer following the sea ice as it retreats.[33] Furthermore, bowhead whales around the Svalbard Archipelago have been observed to be on average ~100 km offshore during the summer.[51] Given that we only used radiocarbon dated fossil records - primarily located along coastlines - to calibrate and validate our ecological models, Svalbard fossils in all likelihood resulted from animals that died in summer.

Previous work has shown that bowhead whales prefer cold, ice-covered water, with individuals spending most of their time in a narrow temperature range > -1°C SST < 1°C, near the marginal ice zone, but also moving into areas with >90% SIC during winter.[51] Proximity to coastline, and consequently, bathymetric depth has also been shown to be an important variable controlling bowhead whale distribution,[51] but we were not able to calculate these metrics (e.g. bathymetric depth, distance from continental shelf) accurately because accurate bathymetric data for our high-resolution palaeoclimate reconstructions do not exist.[138] We included salinity as a proxy for regional differences in ocean productivity, with decreased pelagic and benthic diversity often occuring in areas of lower salinity.[148] Consequently, our estimates of SST, SAL, and SIC metrics could be considered both proximal and distal predictors as they have a direct (proximal) influence on bowhead whale physiology and behaviour (and therefore fitness), and an indirect (distal) influence on prey distributions.

Ecological niche model

We created an ecological niche model (ENM) for bowhead whales using the Hypervolume package for R.[71] We generated best estimates of the ecological niche as a 3-dimensional hypervolume[149] across time.[146] Hypervolumes were constructed using the "Gaussian" hypervolume method,[150] with bandwidths, number of standard deviations, and the probability threshold tuned using independent calibration and validation datasets. Gaussian hypervolumes were built by defining a Gaussian kernel density estimate on an adaptive grid of random n-dimensional points around the original data points. The bandwidth multiplier, number of standard deviations, and the probability threshold all control the size and configuration of the kernel density estimate.[71,150]

Tuning and cross-validation resulted in the optimised hypervolume model having high accuracy as measured by AUC and Boyce Index. Tuning for the hypervolume parameters resulted in our final hypervolumes using a bandwidth multiplier of 1.5, three standard deviations, and a probability threshold of 0.99. 97% of our validation points were also shown to fall within the 3-dimensional boundary of our hypervolume. Our tuned ENM projections had good ability to discriminate between areas of high suitability at our withheld validation sites, relative to background samples (AUC = 0.83; Boyce index = 0.97).

We withheld a stratified 10% of our expanded occurrence records to use as an independent validation set, with the remaining 90% of records used to calibrate the hypervolume. We intersected the 30-year averages for our climate and environmental variables for each georeferenced fossil for the period ± 2 SD around the estimated age of the fossil, ensuring that each fossil record had a time series of climate data associated with it.[151] This time series represents the period over which bowhead whales were likely to have been present near the fossil sites, given inherent dating uncertainty. Before pairing the fossil records with the environmental and climate data (see above) to define the niche, we merged records where there was spatiotemporal overlap within each 1° × 1° grid-cell. To do this, longitude and latitude values for fossils (Table S2) were rounded to one decimal place (retaining ~11.1 km of accuracy) and grouped. Each record was then checked for temporal overlap with all other records in the same group. Temporal overlap was defined as overlapping confidence intervals for the calibrated radiocarbon ages (Calibrated Age ± 2 S.D.). Where temporal overlap occurred, the confidence intervals were merged for all overlapping records resulting in a single record with an expanded age interval. Pre-processing the collated fossil records using this approach reduced the number of records for modelling the niche to 585 (n = 526 calibration, n = 59 validation). Expanding the calibration and validation datasets to their full temporal coverage resulted in 10,798 calibration records and 1,148 validation records.

To characterise the environmental conditions at each fossil location, SST, SIC, and SAL were calculated as the average values from the nearest ocean grid-cell containing the fossil and the 8-nearest cells. The 9-cell averaging approach was chosen to minimise fine-scale artificial accuracy/biases introduced during the bias correction and downscaling of the climate data[138] and to overcome positional uncertainty regarding the potential ocean cells from which the fossils were likely to have arisen. For this process, fossils that were located on land according to the temporally explicit land/sea mask, were snapped to their nearest ocean-cell, up to a maximum distance of 150 km, before the nearest 8-cells to the "new" fossil location were identified (Extended data figure 13).

Climate suitability projections

Spatially and temporally explicit projections of habitat suitability were created at 50-year generational time steps from 11 kya to 0 kya for bowhead whales. We opted to set an upper limit on our hindcasts as only 7% of our fossil record was from fossils older than 11 kya and we therefore had reduced confidence in projections of habitat suitability before this time. Comparisons between spatial projections of habitat suitability from the hypervolume package, and more common maximum entropy methods[152] have shown similar results.[150]

PC1 in the Principal Component Analysis of environmental variables influencing bowhead whale distribution across the Canadian Arctic Archipelago and the Svalbard Archipelago explains 66.2% of the variance, primarily driven by sea surface temperature (SST). PC2 explains 27.4% of the variance, with contributions from salinity and sea ice cover. Furthermore, there is some overlap between the Canadian and Svalbard groups, but they remain distinct, particularly on PC1 (Extended data figure 14).

Fluctuations in habitat suitability were not highly affected by the modelled changes in fractional sea ice cover or variation in SST, suggesting that habitat suitability was a function of all the variables in the hypervolume (Figures 2A–2C and S1; Table S1). Habitat suitability peaked in the Svalbard Archipelago at the onset of the Holocene, but did not peak in the Canadian Arctic Archipelago until ~10-8 kya, when average summer SST was between 1-1.5 °C and summer fractional sea ice cover was between 40% and 50%. The ENM projected a decreasing trend in average habitat suitability from 10.5 kya to ~9.5 kya in Svalbard, however, in the Canadian Archipelago habitat suitability decreased at a slower rate from 10 kya to 5 kya (Figure 2C). After these time periods, habitat suitability fluctuated slightly around a long-term mean. Analysis of the centre of gravity of habitat suitability, indicated a southward shift of up to ~2° in both subpopulations, as habitat suitability decreased (Figure 2D). Animations of habitat suitability through time for the study region are provided as a supplementary video (Video S1).

Throughout the Holocene, suitable habitat for bowheads showed strong connectivity across much of the Arctic (Video S1), including the Russian Arctic where particularly little is known about present-day bowhead whales distribution.[53] Despite a relative lack of contemporary information, and no fossil records from these locations, bowhead whale sightings have been reported from Franz Josef Land.[153] Further east, bowhead whales have also been observed in the western Laptev Sea,[154] and the north of the Novosibirsk Islands Archipelago, which separates the Laptev and East Siberian seas.[155]

Therefore, although our finding of differentiation between contemporary stocks may reflect a recent colonisation by a distinct group of bowhead whales, this is not supported by our other findings. Our habitat modelling suggests that connected suitable habitat was present across the circumpolar Arctic throughout the Holocene and up until the present day (Video S1). Coupling this with the high mobility of bowhead whales, and the fact that Canadian and Svalbard individuals represented a single population throughout the Holocene, despite sampling sites between regions being separated by several thousand km, it seems unlikely a genetically differentiated population existed to recolonise Svalbard. This is also supported by our forward-in-time genomic simulations showing that the commercial whaling induced population bottleneck would lead to increased population differentiation (Figure 4B).

Using the full multi-temporal fundamental niche hypervolume, we used the 10% validation test set to fine-tune the two parameters that affect the probability density (i.e. habitat suitability) of the hypervolume: (i) weight.exponent, and (ii) edges.zero.distance.factor. These two parameters in combination control the rate and distance at which habitat suitability shifts to 0 from its empirical maximum. A grid search was done using both parameters (edges.zero.distance.factor range = 1:10; weight.exponent range = -1:-3), before extracting values of habitat suitability at fossil locations (temporally explicit), and then calculating the Boyce Index and area-under the receiver operating curve (AUC) values.[156,157] The Boyce index is a presence-only evaluation measure used to discriminate how much projections of habitat suitability at presence locations differ from random expectation, with higher Boyce values indicating greater habitat suitability at presence locations than would be expected by chance. Likewise, higher AUC values indicate greater capacity for the hypervolume projections to discriminate between background locations and training/validation sites. Background points for calculating both measures were defined using the background points from the full hypervolume. Final parameters were chosen based on the combination of parameters that maximised the Boyce Index and AUC and consequently habitat suitability at fossil locations through time. Following tuning and validation, the weight.exponent was set to -1 and edges.zero.distance.factor was set to 3. As the outputs of the hypervolume_project function are not bound by [0, 1],[71,150] each of the projections of habitat suitability was then rescaled to the range 0-1 using the 10% training presence threshold (OR10). The OR10 is defined as the threshold which excludes regions with suitability values lower than the values for 10% of training records – the assumption being that the lowest 10% of training records are from regions that are not representative of the species overall habitat and can be omitted. Values were rescaled using the formula:

$$X_r = \frac{x - OR10}{P_{95\%}(x > OR10) - OR10}$$

Where X_r is the rescaled suitability value, x is the original value, OR10 is the 10th percentile omission threshold from the training data, and $P_{95\%}$ is the 95th percentile of all x values > OR10. We opted to rescale based on the 95th percentile of suitability values due to the extreme right skew of the suitability values inflating the maximum value. Projections of habitat suitability were then reprojected using bilinear interpolation to a stereographic polar projection with a resolution of 100 km x 100 km.

Stable isotope analysis

Approximately 100 mg of powdered bone was obtained from each subfossil bowhead whale specimen using a dremel drill and demineralized in 0.5 M HCl for 4 h under constant motion (orbital shaker). The samples were then rinsed with Type I water (18.2 MΩ·cm), treated with 0.1 M NaOH for 20 minutes. This step was repeated until there was no colour change in the solution. The samples were then heated at 75°C for 36 hrs in 3.5 mL 0.01 M HCl to solubilize the collagen, and freeze-dried.

We determined carbon and nitrogen isotopic and elemental compositions using a Nu Horizon isotope ratio mass spectrometer (IRMS) coupled to a EuroVector 3000 elemental analyzer (EA). The δ^{13}C and δ^{15}N values were calibrated relative to the international

Please cite this article in press as: Westbury et al., Four centuries of commercial whaling eroded 11,000 years of population stability in bowhead whales, Cell (2026), https://doi.org/10.1016/j.cell.2026.02.022

reference scales (VPDB and AIR) using USGS40 and USGS41a.[158,159] We assessed measurement uncertainty using three in-house standards with the following established isotopic compositions: SRM-1 (caribou bone collagen, $\delta^{13}C$ = −19.36±0.11 ‰, $\delta^{15}N$ = +1.81±0.11 ‰), SRM-2 (walrus bone collagen, $\delta^{13}C$ = −14.77±0.11 ‰, $\delta^{15}N$ = +15.59±0.11 ‰), SRM-14 (polar bear bone collagen, $\delta^{13}C$ = −13.67±0.07 ‰, $\delta^{15}N$ = +21.60±0.15 ‰), and SRM-15 (phenylalanine, $\delta^{13}C$ = −12.44±0.04 ‰, $\delta^{15}N$ = +3.08±0.12 ‰). To check for homogeneity of the collagen, twenty percent of the samples were analysed in duplicate. Standard uncertainty was calculated to be ±0.14 ‰ for $\delta^{13}C$ and ±0.28 ‰ for $\delta^{15}N$.[160]

In total, we successfully generated bone collagen stable $\delta^{13}C$ and $\delta^{15}N$ isotopes from 196 Holocene specimens (Figure 1B; Table S3). We also generated $\delta^{13}C$ and $\delta^{15}N$ values from four Late Pleistocene individuals (1 from Canada, 3 from Svalbard), but as they are not directly comparable to the Holocene individuals, we excluded them from downstream analyses. When plotting the results through time, we observed no obvious differentiation between genetically identified females and males (Extended data figure E2). Therefore, we did not separate the data by sex in interpretations.

We generated locally estimated scatterplot smoothing (LOESS) trendlines using the statistical software package PAST v4.03[70] with a smoothing factor of 0.25.

Genomics

Ancient DNA data generation

We obtained ∼50 mg of bone powder from each subfossil bowhead whale specimen using a dremel drill for DNA analyses. We extracted DNA from the bone powder using a modified version of a previously published protocol.[161] Modifications included using a modified version of the Qiagen PB binding buffer[162] and concentrating the extraction supernatant to ∼100ul using Amicon spin columns prior to purification. We measured the DNA concentration in the extracts using the Qubit high sensitivity kit. We performed a full USER enzyme treatment step to remove uracil residues from damaged DNA and the resultant abasic sites.[163] We built Illumina sequencing libraries from the USER treated extracted DNA following the BEST protocol,[164] with 1uL of a predetermined Illumina adapter mix concentration (1 - 50 uM) based on the DNA extract amount (Extended data table 7) and a set number of indexing PCR cycles, predetermined a priori through a qPCR reaction.

Index PCR was performed using dual-indexing and libraries were combined into pools of ∼50 unique indices. Index reactions were performed using the Kapa Hifi Uracil + Readymix and the following PCR conditions: 98°C for 45 seconds, then 98°C for 15 seconds, 60°C for 30 seconds, and 72°C for 20 seconds for the number of cycles predetermined via qPCR, and finally a cool down to 10°C. We sequenced each library pool on a single Illumina Hiseq 4000 lane at the GeoGenetics Sequencing Core, University of Copenhagen using 80 bp single end (SE) chemistry. We selected individuals for deeper sequencing based on endogenous DNA content (number of unique mapped reads/total number of raw reads), age, and locality. We built additional sequencing libraries for the selected samples following the same protocol as above, which were sequenced on an Illumina Hiseq 4000 with 80 bp SE chemistry.

We enriched 34 Svalbard individuals for mitochondrial genomes using RNA baits based on the published bowhead whale mitochondrial genome (Genbank accession: KY026773.1). Enrichment was performed using the hybridization capture myBaits Custom DNA-Seq kit (Arbor Biosciences). Following myBaits recommendations, we used between 150 – 280 ng of starting material of each indexed library for every capture reaction. The capture procedure was carried out as described in the myBaits manual v.5.00; we used the High Sensitivity conditions, which are optimised for ancient samples, with a hybridization step at 55 °C for 24 h. Post-capture, the libraries were re-amplified using Kapa Hifi Uracil + Readymix and the following PCR conditions: 98 °C for 45 minutes, then 98 °C for 20 seconds, 60 °C for 30 seconds, and 72 °C for 45 seconds for 14 cycles, and a final elongation at 72 °C. Re-amplified libraries were quantified and quality checked as described above. Sequencing was carried out on a NovaSeq 6000 at Novogene Europe with 150 bp PE chemistry.

Contemporary genomic data generation

We extracted DNA from the seven contemporary Canadian individuals using a DNeasy blood and tissue kit (Qiagen) following the manufacturer's protocol. We fragmented the extracted DNA to an average length of ∼450 bp using a M220 Focused-Ultrasonicator™ (Covaris). We built Illumina sequencing libraries from the fragmented extracts using the BEST protocol,[164] with an Illumina adapter mix concentration of 20uM, and 15 cycles during the indexing PCR step. We cleaned the indexed libraries using a SPRI bead DNA purification method. Each indexed library was sent to Novogene for 10 Gb of 150 bp paired end (PE) sequencing on a Novaseq Illumina platform.

Data processing

For the 202 subfossil individuals that successfully produced sequencing data, we trimmed adapter sequences and removed reads shorter than 30 bp from the raw reads using skewer v0.2.2.[73] We mapped the trimmed reads to the bowhead whale reference genome (http://www.bowhead-whale.org/[165]) including the mitochondrial genome (Genbank accession: KY026773.1) using Burrows-wheeler-aligner (BWA) v0.7.15[75] utilising the aln algorithm, with the seed disabled (-l 999) (otherwise default parameters). We parsed the alignment files and removed duplicates and reads of mapping quality score <30 using SAMtools v1.6.[76] We checked for ancient DNA damage patterns using mapDamagev2.[77]

Of the 202 individuals, a total of 44 individuals had nuclear genome-wide coverages ranging from 0.20x-3.45x, comprising 33 from Canada and 11 from Svalbard (Table S4). Individuals had typical ancient DNA damage patterns, with elevated C-T transitions on the 5-prime end of the reads, and elevated G-A transitions at the 3-prime end of the reads (Extended data figure 15).

We generated a total of 107 complete mitochondrial genomes (>10x) from the fossil material. All 65 Canadian mitogenomes and 20 of the Svalbard mitogenomes were obtained via shotgun sequencing. An additional 22 Svalbard mitogenomes were obtained via target enrichment. We were also able to generate mitochondrial genomes from three of our four Late Pleistocene samples: CGG_1_023629, CGG_1_023776, CGG_1_023745. The mean coverages of the mitogenomes ranged between 10x and 271.45x (Table S4).

All samples that yielded mitochondrial genomes were confirmed to be bowheads based on similarity to the reference genome and to each other, validating previous identifications. An overview of the individuals used in the mitochondrial and nuclear genomic analyses is found in Extended data table 6.

For the 19 contemporary individuals (Canada n = 7, Svalbard n = 12), we trimmed adapter and poly-G sequences and removed reads shorter than 30 bp from the raw reads and merged overlapping paired-end reads using Fastp v0.20.1.[74] We mapped both merged and unmerged reads to the bowhead whale reference genome using BWA with the mem algorithm (otherwise default parameters). We parsed the alignment files and removed duplicates and reads of mapping quality score <30 using SAMtools. This resulted in partial- and low-coverage genomes (0.23x - 1.24x) from seven contemporary 'East Canada-West Greenland' stock bowhead whales, and higher coverage (9.96x - 20.94x) for the downloaded published data from the twelve contemporary 'East Greenland-Svalbard-Barents Sea' stock individuals (Table S5). Our seven contemporary Canadian samples all yielded complete mitochondrial genomes (496.8 - 3902.5x).

Combining this with 15 available Svalbard samples,[22,166] we had a total sample size of 110 Holocene fossils and 22 contemporary mitogenomes.

Nuclear genomes

We found putative sex chromosome scaffolds in the bowhead whale reference genomes by aligning it to the Cow X (Genbank accession: CM008168.2) and Human Y (Genbank accession: NC_000024.10) chromosomes. We performed the alignments using satsuma synteny v2.1[78] with default parameters.

Relatedness

We assessed whether any of our contemporary individuals could be closely related to each other using NGSrelate v2.[167] As input for this we calculated genotype likelihoods for the contemporary individuals using ANGSD v0.921.[79] We calculated genotype likelihoods using the GATK algorithm (-GL 2), specified the output as a binary beagle file (-doGlf 3), and applied the following filters: only include reads with a mapping quality greater than 20 (-minmapQ 20), only include bases with base quality greater than 20 (-minQ 20), only include reads that map to one location uniquely (-uniqueonly 1), a minimum minor allele frequency of 0.05 or greater (-minmaf 0.05), only call a SNP if the p-value is less than $1e^{-6}$ (-SNP_pval 1e-6), infer major and minor alleles from genotype likelihoods (-doMajorMinor 1), skip triallelic sites (-skipTriallelic 1), remove sex scaffolds and scaffolds shorter than 100 kb (-rf), and call allele frequencies based on a fixed major and an unknown minor allele (-doMaf 2). We determined a relatedness coefficient (RAB) >0.125 (equivalent of first cousins) as closely related.

When considering a relatedness coefficient score (RAB) >0.125, equivalent to first cousins, as our cut off for closely related individuals, we did not find any closely related individuals in our contemporary genomes. This is in line with previous findings,[22] that also did not find closely related individuals in the same 'East Greenland-Svalbard-Barents Sea' individuals.

Sex determination

We calculated the average coverage of scaffolds aligning to the X chromosome and the autosomes (scaffolds not aligning to either the X or the Y chromosome) using SAMtools depth. We determined the sex of an individual by calculating the X:A, the ratio of coverage on the X scaffolds to the autosomal scaffolds. Of the 202 individuals analysed, 16 subfossil individuals had <5,000 mapped reads and were not considered further for sex determination analysis.[80] If an individual had an X:A ratio of <0.7 it was designated as a male. If an individual had an X:A ratio of >0.8 it was designated as a female. Individuals with ratios between 0.7 and 0.8 were deemed undetermined.[80] To investigate changes through time, we subsequently pooled individuals into 1,000 year time bins and calculated the ratio of males to females.

Genetic sexing showed the Holocene dataset of 202 individuals contained 100 females, 83 males, and 19 individuals with undetermined sex. The proportions of females to males in our dataset was relatively consistent through time at ~6:4 (Extended data figure 16), although the proportion from the Canadian samples and the Svalbard samples varied. Of the 109 specimens available from the Canadian Arctic Archipelago, we genetically identified 45 as female, 61 as male, and 3 were undetermined. Of the 93 available specimens from the Svalbard Archipelago, we genetically identified 55 as female, 22 as male, and 16 were undetermined. Information on individual genetic sexing is provided in Table S4. We did not genetically sex the contemporary samples.

Population structure

We investigated population structure by computing covariance matrices for Principal Component Analyses (PCA) using PCAngsd v0.95[81] using all individuals with >0.2x genome-wide coverage. As the input for PCAngsd, we generated a genotype likelihood beagle file in ANGSD using the following parameters: -minmapQ 30, -minQ 30, -GL 2, -doGlf 2, -doMajorMinor 1, remove transitions (-rmtrans 1), -doMaf 2, -SNP_pval 1e-6, -minmaf 0.1 -skiptriallelic 1, -uniqueonly 1, only include sites where at least 40 individuals have coverage (-minind 40), only including autosomal scaffolds >100kb (-rf).

We tested the robustness of our PCA results to coverage and aDNA damage patterns by repeating the analyses with modified versions of the 12 high-coverage contemporary 'East Greenland-Svalbard-Barents Sea' individuals, while keeping all factors, including parameters, unmodified. To test the impact of coverage, we downsampled all 12 contemporary 'East Greenland-Svalbard-Barents

Please cite this article in press as: Westbury et al., Four centuries of commercial whaling eroded 11,000 years of population stability in bowhead whales, Cell (2026), https://doi.org/10.1016/j.cell.2026.02.022

Sea' individuals to ~2x using SAMtools. To test the impact of shorter read lengths and aDNA damage patterns, we trimmed the forward reads of the 12 individuals to 80 bp using skewer, and simulated aDNA damage patterns on the ends of the reads, using TAPASv1.2,[83] based on the mean damage misincorporation values generated by mapDamagev2 from all ancient bowhead samples. We mapped the simulated aDNA reads back to the bowhead whale reference genome using the same parameters as implemented for the ancient specimens. Finally, we downsampled the aDNA simulated individuals to 1x using SAMtools. We computed the genotype likelihoods in this aDNA simulated dataset in ANGSD using the same filtering as for the complete dataset and computed PCAs using covariance matrices from PCAngsd. This resulted in three additional PCA runs: 1) Contemporary EGSB samples downsampled to ~2x coverage, fossil and ECWG individuals remained unchanged, 2) Contemporary EGSB samples have ancient DNA damage patterns simulated onto the reads as well as and reduced read lengths (80bp), fossil and ECWG individuals remained unchanged, 3) Contemporary EGSB samples have ancient DNA damage patterns simulated onto the reads as well as and reduced read lengths (80bp) and are downsampled to 1x, fossil and ECWG individuals remained unchanged.

We extracted the 2,280,657 transversion SNP sites remaining after filtering the aDNA simulated dataset (all ancient individuals >0.2x, all contemporary 'East Canada-West Greenland' individuals, and the simulated aDNA damaged 'East Greenland-Svalbard-Barents Sea' individuals), which we term as the population SNP panel.

Finally, using the population SNP panel, we reran the original analysis (all ancient individuals >0.2x, all contemporary 'East Canada-West Greenland' individuals, and all 'East Greenland-Svalbard-Barents Sea' individuals) using both genotype likelihoods and pseudohaploid base calls (-doIBS 2 and -doCov 1 in ANGSD) as well as a genotype likelihood PCA using only the subfossil individuals. We determined the significance of the Principal component axes using a Tracy-Widom test on the eigenvalues in R.[168,169] A significant value was determined based on $p<0.01$.

The PC1 axis clustered all 44 Holocene fossil samples together, regardless of geographic origin, while the 19 contemporary Canadian and 'East Greenland-Svalbard-Barents Sea' individuals formed unique clusters (Figure 3B). We retrieved similar results when downsampling the 12 contemporary 'East Greenland-Svalbard-Barents Sea' individuals to 2x, as well as simulating ancient DNA damage on the 'East Greenland-Svalbard-Barents Sea' individuals and downsampling these genomes to 1x (Extended data figures 6-14). When computing a PCA with only Holocene fossil samples, one individual became separated from all others on the PC1 axis (Extended data figure 11). When plotting the PC1 and PC2 axes, PC2 highlights variation among contemporary individuals sampled from the 'East Greenland-Svalbard-Barents Sea' stock (Extended data figure 17). Further investigations into the significance of the principal components using a Tracy Widom test showed that only PC1 was significant when including both fossil and contemporary individuals, while when only including fossil individuals, no PC was significant. We found consistent results between using genotype likelihoods and pseudo haploid base calls (Extended data figure 18).

Using the same genotype likelihoods computed for the PCA with the population SNP panel, we calculated admixture proportions in our dataset using NGSadmix[82] specifying K=2, 3, and 4. To determine convergence in our dataset, we repeated the analysis up to 50 times per K value. If two runs produced the same likelihood values then we classified this as converging. Out of the three investigated K, only K=2 converged indicating only this value is suitable for our data. The result for K=2 shows the contemporary 'East Greenland-Svalbard-Barents Sea' individuals to have the most unique ancestry (Extended data figure 19). Despite not converging, we also investigated the replicate with the highest likelihood for K=3 (Extended data figure 19). Results do not show a clear pattern of population structure in space or time, suggesting there is only one main set of differentials in the dataset.

We quantified the levels of genetic divergence between pre-whaling and post-whaling bowhead whales and between localities using fixation index (F_{ST}) values. Despite the PCA analysis suggesting a single panmictic population in our Holocene subfossil individuals, to further investigate this, we chose to pool individuals into one of four populations; pre-whaling Canada, pre-whaling Svalbard, post-whaling Canada, post-whaling Svalbard. We created a consensus pseudohaploid base call (-dohaplocall 2) file using the population SNP panel (-sites) in ANGSD. We calculated F_{ST} in 500 kb non-overlapping sliding windows, with a minimum requirement of 100 (variant) sites per window using the available popgenWindows.py (https://github.com/simonhmartin/genomics_general).

Overall, F_{ST} values were very low. All comparisons had mean F_{ST} values >0, but the distribution of F_{ST} values across the genomes overlapped with 0 (Extended data figure 5). When comparing Holocene individuals from Canada and Svalbard, we obtained a mean F_{ST} of 0.002. When comparing contemporary individuals from the same regions, we obtained a mean F_{ST} of 0.007.

Genome-wide SNP heterozygosity

It has been suggested previously that genome-wide SNP heterozygosity can be estimated relatively accurately in very low-coverage individuals (<1x) when using genotype likelihoods and sites with common variants (minor allele frequency >0.1).[170] We tested this with our dataset by calculating genome-wide SNP heterozygosity independently, five times, on three different high-coverage 'East Greenland-Svalbard-Barents Sea' individuals, with different simulated treatments using the population SNP panel. The SNP panel had rare variants (minimum minor allele frequency 0.1), transition polymorphisms, and monomorphic sites removed. Treatments included (i) no treatment (i.e. the full high-coverage dataset), (ii) the same dataset downsampled to 2x, (iii) R1 reads trimmed to 80 bp and the addition of aDNA damage patterns, (iv) R1 reads being trimmed to 80 bp, the addition of aDNA damage patterns, and downsampled to 1x, and (v) trimmed R1 reads to 80 bp, the addition of aDNA damage patterns, and downsampled to 0.2x. The simulated aDNA damage was added using TAPAS as described above for the PCA tests.

We calculated genome-wide SNP heterozygosity for each individual independently for the filtered sites using genotype likelihoods in ANGSD with the following parameters: -minmapQ 30 -minQ 30 -doCounts 1 -GL 2 -doMajorMinor 1 -rmtrans 1 -doMaf 2 -skiptriallelic 1 -uniqueonly 1, compute sample allele frequencies (-doSaf 1), compute a folded SFS (-fold 1), reduce all sites with >2x

coverage to 2x (-capdepth 2). We computed a folded SFS from the sample allele frequencies using realSFS, part of the ANGSD toolsuite. To fold the SFS we used the reference genome as both the -ref and -anc parameters. To calculate the variance in our results we randomly sampled 500 thousand sites from our SNP panel 20 times, and independently calculated genome-wide SNP heterozygosity for each individual using each of the 20 subsampled SNP panels. Based on our results, we proceeded to calculate the genome-wide SNP heterozygosity for all individuals in our dataset >0.2x following the same protocol and restricted our genome-wide SNP heterozygosity estimates to sites in the population SNP panel. Furthermore, as our tests on the impact of aDNA damage showed a bias towards higher genome-wide SNP heterozygosity in specimens with ancient DNA damage, we compared the pooled results (both original coverage and downsampling) obtained from the undamaged individuals (17-07, 17-12, and 17-19) to the pooled results from the same individuals with aDNA damage simulated to calculate the average difference. We subtracted the average difference (0.008) from the values obtained for our empirical Holocene fossil specimens (Extended data figure 1). Although we saw increased within individual variation when downsampling the aDNA damage simulated individuals from 1x to 0.2x, the majority of samples investigated were >1x (30/44), with 0.2x only being the minimum cutoff. Therefore, our overall results should not be highly influenced by this increased variation at very low coverages. We note that our results represent SNP heterozygosity, and therefore should only be relatively compared between individuals analysed with the same SNP panel.

Downsampling coverages did not appear to cause large deviations in mean heterozygosity but did increase variation in the results, especially when downsampling from 1x to 0.2x. However, when simulating ancient DNA damage, we saw a noticeable increase in heterozygosity. The mean deviation between contemporary and ancient simulated samples was 0.008. We did not observe any obvious associations between sequencing depth and heterozygosity estimates (Extended data figures 20 and 21; Extended data table 8).

We tested for significant differences between all pre-whaling Holocene specimens (since population structure results suggest that they were a single panmictic population), contemporary 'East Canada-West Greenland' stock specimens and contemporary 'East Greenland-Svalbard-Barents Sea' stock specimens by pooling the 20 subsampled genome-wide SNP heterozygosity estimates from all individuals in the given bin together and performing a Mann-Whitney-Wilcoxon Test in R v4.1.1.[72]

Genome-wide nucleotide diversity

We investigated nucleotide diversity through time by splitting our dataset of individuals with >0.2x coverage into 1,000 year time bins. As the PCA suggested a single panmictic population in the pre-whaling Holocene, we kept contemporary Canada and contemporary Svalbard bowhead whales as two separate populations, but pooled the ancient individuals from the two regions to increase sample size in the pre-whaling Holocene time bins. We created a consensus pseudohaploid call (-dohaplocall 2) file in ANGSD at the sites in the population SNP panel (-sites parameter) and using the following filters; -doMajorMinor 1 -rmtrans 1 -doMaf 2 -SNP_pval 1e-6 -minmaf 0.1 -skiptriallelic 1 -uniqueonly 1 -minind 40. We estimated nucleotide diversity from the pseudohaploid call file in 500 kb non-overlapping sliding windows, with a minimum requirement of 100 sites per window using the popgenWindows.py (https://github.com/simonhmartin/genomics_general). We assessed the significance of differences between the bins using a Mann-Whitney-Wilcoxon Test in R v4.1.1.[72] We used a Bonferroni correction to identify the threshold for significance (p-value of 0.05/6038 windows), giving us an upper p-value for significance of 0.000008.

We observed similar levels of nuclear nucleotide diversity (π) across the subfossil time bins. The majority of comparisons based on the fossil data (samples >500 years old), did not produce significant differences in diversity levels, with mean values ranging from 0.362 to 0.366 (Figure S2; Extended data table 3). However, we did observe significantly lower levels of nucleotide diversity (Extended data table 3) in the contemporary 'East Greenland-Svalbard-Barents Sea' individuals (0.355 +/-0.035) relative to the pre-whaling time bins, and also relative to contemporary Canada (0.366 +/- 0.042). In contrast, the diversity of contemporary Canadian individuals was not significantly different to the pre-whaling time bins.

Simulating bottleneck impact on genetic diversity estimates

We used an Approximate Bayesian Computation (ABC) approach to infer levels of commercial whaling associated population decline. The principle of ABC methods relies on running simulations over a wide range of parameters under a specific model to find those parameter values that generate datasets that most closely match the observed data.[171] We simulated data using msprime.[87] We used uniform distributions for key demographic parameters to explore a broad range of demographic models. We modeled a scenario where an ancestral population split into two populations (corresponding to Canada and Svalbard) T_a generations ago. These populations then were allowed to experience an instantaneous bottleneck T_b generations ago, reducing their sizes. Our model also accounted for asymmetrical gene flow both before and after the divergence.

The divergence time between the two populations was drawn from a uniform distribution ranging from 200 to 5,000 generations, sampled at 100-generation intervals. Ancestral effective population sizes for both Canada and Svalbard were sampled from a uniform distribution ranging from 1,000 to 10,000. We aimed to infer the intensity of the bottlenecks, defined as the proportional reduction in effective population size (N_e) and estimated as the ratio of present to past population sizes. Therefore, we set the prior of this ratio to a wide uniform distribution varying between 0 and 99%, representing virtually no change in size to a strong bottleneck. We varied T_b, the time of the bottleneck, between 12 to 16 generations before present. Migration rates were allowed to vary before and after the bottleneck, ranging from 0 to 5 migrants per generation.

We performed 1,000,000 simulations by randomly drawing parameter values from the priors. The simulated data were summarized using two genetic statistics informative about within-population diversity and between-population differentiation, which were available in the empirical dataset. Specifically, we estimated i) genetic diversity (π), the mean number of pairwise differences between

individuals in each ancestral and present-day population, and ii) F_{ST} pre-bottleneck and post-bottleneck. We then calculated the ratios between pre-bottleneck and post-bottleneck values for each of these summaries. We used a rejection ABC approach, where the Euclidean distance between the simulated and observed data was computed based on three summary statistics: F_{ST} pre-/post-bottleneck, π Canada pre-/post-bottleneck, π Svalbard pre-/post-bottleneck. These three ratios were treated equally and combined into a single Euclidean distance metric. Among the one million simulated datasets, we retained the 10,000 simulations (1%) with the smallest Euclidean distances, i.e., those considered closest to the empirical data according to these three summary statistics.

The posterior estimates of the putative population size change varied between the Canada and Svalbard populations. In the case of the Svalbard, the inferred posterior favored a clear bottleneck (a peak in posterior value at ~0.92), whereas no bottleneck was observed in Canada (Figure 4A). For Canada, the prior did not clearly differ from the posterior, and was wide and relatively flat, suggesting that there isn't enough information in the data to clearly support a bottleneck signal. The migration rates prior to the whaling-induced bottleneck did not show significant deviation from the prior distribution, indicating no particular migration pattern was favored. In contrast, for the post-whaling migration rates, the posterior exhibited a shift towards higher values suggesting migration in our tested models. Due to the lack of support for any specific pre-whaling migration rate, we cannot conclusively determine whether migration rates increased or decreased post-whaling.

To infer the long-term impact of the bottlenecks, we performed forward-in-time simulations of neutral and deleterious variation using SLIM3,[88] parametrized with the most likely bottleneck intensities obtained from ABC. These simulations aimed to estimate the future response of genome-wide diversity and fitness loss under different demographic recovery scenarios. We used the best estimated proportional reduction in N_e of 92% for the Svalbard population. Since the ABC method did not resolve the bottleneck intensity for Canada, we applied a conservative decline of 48%. Simulations were run using a non-Wright-Fisher model with random mating and overlapping generations to allow faster execution.

We simulated two ancestral populations of different sizes based on pre-whaling estimates of the 'East Greenland-Svalbard-Barents Sea' stock (52,500 individuals)[12] and the 'East Canada-West Greenland' stock (~18,500 individuals).[14] We converted population size into effective population size by dividing by 10,[172] resulting in N_e=5,250 and N_e=1,850. The ancestral populations exchanged five individuals per generation to simulate the low level of differentiation observed in ancient genomes. To initialize the simulations, we first generated a tree sequence in msprime representing the ancestral (meta)population at mutation-drift equilibrium for neutral mutations. This tree sequence was then used as input to SLIM3, where we introduced deleterious mutations and simulated forward in time for 2,000 steps to allow the system to reach a mutation-drift-selection equilibrium. We confirmed equilibrium by monitoring stable trends in genome-wide nucleotide diversity and genetic load prior to initiating bottleneck scenarios.

As bowhead whales have long generation times (35-50 years, [22]), and commercial whaling occurred within the last ~500 years, we simulated the bottlenecks 15 generations ago (corresponding to 525 years ago). After the bottleneck, we simulated two scenarios: no migration or one migrant per generation. We modeled several demographic recovery scenarios starting from the present day to explore how populations might rebound following bottlenecks. These scenarios included trajectories where the population either remained at its reduced post-bottleneck Ne, or gradually recovered to 25%, 50%, 75% or 100% of its pre-whaling N_e. Recovery was simulated by doubling the population size each generation until reaching the specified recovery percentage. A doubling of population size each generation reflects empirically observed growth rates of ~3-4% per year in bowhead whale populations, specifically the ECWG and Bering-Chukchi-Beaufort stocks[173,174]

We simulated neutral and deleterious mutations at relative proportions of 1:2.3 with selection coefficients drawn from a gamma distribution, a 5% lethal tail, and a negative relationship between selection and dominance coefficients as implemented in Kardos et al.[175] We simulated an exome architecture of 20,000 genes of 600 bp each with a recombination rate of $1e^{-04}$ per base-position per generation (to reduce strong background selection), no recombination within genes and a mutation rate of $2.77x10^{-08}$.[176] This resulted in a realistic amount of genetic load (mean = 5.2, sd = 0.4 lethal equivalents), within the range of lethal equivalents estimated for mammals.[177] We estimated different genomic metrics through time; average genome-wide heterozygosity per population, genetic differentiation (F_{ST}) between populations and the amount of expressed genetic load (realized load) and its effect on fitness per population using formulas from Bertorelle et al.[52] In our simulations, the realised load (RL) determines individual fitness, and it quantifies the severity of inbreeding depression. We converted the realised load to mean population fitness as e^{-RL}, following Bertorelle et al.[52]

Simulated future scenarios indicate that F_{ST} between populations will remain higher compared to pre-whaling levels, even if migration continues at high rates - comparable to those observed after the bottleneck. F_{ST} will likely continue to increase over the next ~1,000 years under the various 'recovery' scenarios (Figure 4B). This suggests that the intense genetic drift caused by the population collapse alone is sufficient to drive the increase in F_{ST} values. Moreover, the drift debt ensures that this effect persists long into the future. Simulated future scenarios show that diversity will continue to decrease over the next millenia, irrespective of population recovery or migration efforts (Figure 4C). While any level of population recovery can halt the decline in fitness for both populations, even with a complete recovery to 100% of pre-whaling population sizes, fitness levels never return to their pre-whaling state (Figure 4D).

Allele changes correlating with time

As input for Ohana,[84] we created a genotype likelihood beagle file for all Holocene fossil individuals with >0.2x (-doGlf 2) using ANGSD and the following parameters; -minmapQ 25, -minQ 25, -uniqueonly 1. We used the GATK algorithm to call genotype likelihoods (-GL 2), calculate per-site allele frequencies assuming a fixed major and unknown minor allele (-doMaf 2), calculated major and minor alleles using GL (-doMajorMinor 1), minor allele frequency of 0.05 (-minmaf 0.05). This resulted in 12,926,345 sites.

The genotype likelihoods of all individuals were converted to lgm as the input for Ohana using the convert function bgl2lgm. We used qpas to estimate the ancestral component proportions matrix Q (number of individuals x number of ancestral components) and allele frequencies matrix F (number of ancestral components x number of SNPs) from the genotype matrix (lgm) file with the number of ancestral components (-k) ranging from 2 to 6 with an iteration stopping criteria from log likelihood difference (-e 0.0001). In the end, we scanned for selection in each ancestral component while taking into account the sample age as a vector using neoscan. We converted the lle_ratio scores to p-values under a mixture of chi-square distributions,[178] and found the best-fitting genome-wide parameters of the mix using a Kolmogorov-Smirnov test in R.

To evaluate the power of this method and our empirical dataset to uncover alleles undergoing allele frequency changes significantly correlated with time, we simulated a comparable dataset under neutrality and performed the same analysis as with the empirical data. We used the coalescent simulator msprime[179,180] to generate neutrally evolving genetic data for samples that match the empirical data in this manuscript. We ran a demographic model taking into consideration the two pre-whaling populations described in the manuscript (pop1_Ne = 5,250, pop2_Ne = 1,850, generation time = 35, migration rate = 5, recombination rate = 1e-08, mutation rate = 2.77e-08, population split time = 15, 000 years), the sample sizes for each, and the sample ages. We simulated mutations across a 10 Mb genomic region and generated a genotype matrix. This matrix was then the input for simGL (https://github.com/RacimoLab/simGL) to simulate genotype likelihoods, accounting for variable coverage among samples and error rates of 0.00316 based on the minq 25 used in the other analyses. Coverage for each site was modelled as a Poisson distribution with a lambda value corresponding to the average coverage per individual. The resulting genotype likelihoods were converted to beagle format and analysed using Ohana, following the same procedure as before. We investigated 2000 percentiles (between 0 - 100 in 0.05% increments) and produced a QQplot of the percentile results of the empirical data versus the simulated data. We found the simulated data to have lower p-values relative to the empirical data in higher percentiles > 90% (Extended data figure 22). Therefore we concluded that we did not have sufficient power in our empirical dataset to infer the significance of sites that underwent changes in allele frequency correlated with time.

Recent demographic history from modern genomes

We attempted to reconstruct the recent demographic history of the 'East Greenland-Svalbard-Barents Sea' stock using genetic optimization for N_e estimation (GONE)[86] using the 12 high coverage contemporary genomes. As input we generated a PLINK file using the largest 150 autosomes in ANGSD (-doplink 2) with the following parameters -uniqueOnly 1 -GL 2 -remove_bads 1 -minMapQ 20 -minQ 20 -SNP_pval 1e-6 -skipTriallelic 1 -doMaf 2 -domajorminor 1 -minmaf 0.05 -dopost 1 -doplink 2 -minInd 12.

We ran the GONE software using two different parameter sets, one with the default parameters, but with the maximum number of SNPs per scaffold as 10000, and the other with the same parameters but with additional changes in the NGEN and NBIN parameters to 1000 as previously suggested.[181] Each of the parameter sets were run for 100 replicates. We calculated the mean and 95% confidence intervals from these replicates in R.

When running GONE to infer the recent demographic history of the high coverage EGSB individuals, we saw similar patterns regardless of parameter choice, either default parameters or using the parameters from Kardos et al.[181] However, default values produced slightly higher N_e values. When using default parameters, we saw a relatively stable N_e of $\sim 4e^6$ up until $\sim$5 generations ago when it drops to $\sim 3.5e^6$. When using the parameters from Kardos et al.[181] we see a relatively stable N_e of $\sim 3.5e^6$ up until $\sim$5 generations ago when it drops to $\sim 3e^6$. Although the method does capture a decrease in N_e approximately coinciding with commercial whaling, the N_e values are much higher than would be expected based on what has previously been calculated for the pre-whaling population sizes of this stock (52,500 bowhead individuals).[12] This unrealistically high N_e leads us to caution the applicability of this method for our bowhead whale dataset.

We evaluated whether our low-coverage contemporary ECWG samples could produce a reliable site frequency spectrum (SFS) to be used in demographic analyses that require this as input (e.g. stairway plots[182] or fastsimcoal[183]). To do this, we calculated the SFS for our high-coverage EGSB individuals and compared it to one generated after downsampling the same individuals to $\sim$2x. We downsampled using SAMtools. We calculated the SFS from allele frequencies using ANGSD and the parameters: count allele frequencies (-dosaf 1) -uniqueOnly 1 -GL 2 -remove_bads 1 -minMapQ 20 -minQ 20 -skipTriallelic 1 -doMaf 2 -domajorminor 1 -minInd 12. We polarised the SFS using a right whale (*Eubalaena glacialis*) individual (NCBI BioSample: SAMN32746534) as the ancestral sequence (-anc). We mapped the right whale individual to the bowhead whale reference genome using the same approach as for the contemporary bowhead whales. We converted allele frequencies into the SFS using winsfs v0.7.[85]

Investigations into the reliability of the site frequency spectrum obtained from low coverage data ($\sim$2x) revealed a mismatch between values obtained for high coverage individuals, and those same individuals downsampled to 2x (Extended data figure 23). Specifically, we see a loss in low frequency alleles in the downsampled data even when using winsfs, a method that should alleviate some of the bias due to low coverage.

Mitochondrial genomes

We generated mitochondrial genome consensus sequences for Late Pleistocene, pre-whaling Holocene and contemporary individuals using a consensus base call approach (-dofasta 2) in ANGSDv0.921[79] for each individual independently, using the following parameters; minimum base and mapping qualities of 25 (-minmapQ 25, -minQ 25), only include reads that map to a single site uniquely (-uniqueonly 1), minimum read depth of 5 (-mininddepth 5), and build the consensus sequence only for the mitochondrial genome (-r KY026773.1). Only individuals with an average coverage of at least 10x (Late Pleistocene = 3, pre-whaling Holocene = 104,

Please cite this article in press as: Westbury et al., Four centuries of commercial whaling eroded 11,000 years of population stability in bowhead whales, Cell (2026), https://doi.org/10.1016/j.cell.2026.02.022

contemporary = 19) were included in further analysis. We also downloaded three mitochondrial genomes from contemporary Svalbard individuals recently confirmed to have come from unique individuals; individuals named A, H and I.[22]

Mitochondrial nucleotide diversity

To investigate changes in genetic diversity through the Holocene, we estimated nucleotide diversity (π)[184] with DnaSP v.6.12.03[89] for each sampling area for every 1,000 year time bin. We pooled samples from Canada and Svalbard for the ancient specimens but kept contemporary populations separate. We excluded gaps and missing data from the analyses.

All time bins except contemporary Svalbard (haplotype diversity of 0.993) had haplotype diversities equal to 1 (Extended data table 9). Furthermore, unlike with the nucleotide diversity estimates based on the nuclear data, we observed fluctuations in levels of mitochondrial nucleotide diversity through time in the mitochondrial data, albeit with highly overlapping standard deviations (Figure S2B). We observed the lowest levels of nucleotide diversity between 5-4 kya and 2-1 kya. Contemporary individuals do not show lower levels of mitochondrial nucleotide diversity than the Holocene individuals.

Population structure

We constructed an unrooted haplotype network for all complete mitochondrial genomes (Late Pleistocene, pre-whaling Holocene, contemporary) individuals using the Median-joining network[185] as implemented in PopART.[90] Fixation index values (F_{ST}) were calculated by pooling individuals into 2,000 year time bins and splitting them into their two respective regions using Arlequin v3.5,[91] using default parameters and an input file generated with DnaSP. P-values were calculated using 1000 permutations and a significance was defined as a p-value < 0.05.

Haplotype network analyses did not show any spatial or temporal subdivision (Figure S6). Seven haplotypes were shared either across space or across time; four haplotypes were shared between Canada and Svalbard, and one haplotype was shared among three Canadian individuals spanning 12,000 years. The three Late Pleistocene individuals fit within the diversity of Holocene/contemporary individuals. Investigations into Fst values compared between regions and by pooling individuals into 2,000 year time bins revealed no significant differences.

Demographic history

We inferred the changes in female effective population size ($Ne_{(f)}$) through time employing the Bayesian skyline plot method[186] implemented in BEAST v.2.6.1.[93] Based on the network (Figure S6) and F_{ST} analyses of our 107 complete mitochondrial genomes, which spanned >30,000 years in age, we do not see any evidence for population structure, and thus we treated all the data as a single population. We aligned the mitochondrial genomes of all individuals and extracted 38 regions, including protein-coding regions, rRNAs, tRNAs and the control region, based on published coordinates. The sequences of these 38 regions were combined into six subsets, (i) first, (ii) second, and (iii) third codon position of the protein-coding regions, (iv) tRNAs, (v) rRNAs, and (vi) the control region. The best-fit partitioning scheme and substitution model for the six subsets were identified employing Partitionfinder v.2.1.1.[92] The best partitioning scheme and substitution models based on the corrected Akaike Information Criterion were employed as input for Beast2.

The six partitions were analysed using unlinked substitution models that had a linked genealogy and molecular clock. We used tip dates based on the mean calibrated age of each specimen. Five groups of coalescent intervals and a strict molecular clock were assumed. Posterior distributions of parameters were estimated using MCMC sampling, which consisted of 500,000 burn-in steps followed by 500 million steps, sampled at every 10,000 steps. Convergence to stationarity and mixing were assessed using Tracer v.1.7.1[94] and by running an independent replicate with a different seed. Both runs converged to the same joint density or posterior. A minimum effective sample size of 400 was obtained for all the parameter estimates.

Our skyline plot calculated using the entire mitochondrial genome dataset of 129 individuals including Late Pleistocene, Holocene, and contemporary individuals shows maternal effective population size (N_{ef}) across the past 50 ky (Extended data figure 24). N_{ef} was relatively low and stable until the onset of the Last Glacial Maximum ~24 kya, when we observe a rapid and continual increase until ~14 kya. After the peak in N_{ef} ~14 kya, there is a gradual decline until the present, with estimated N_{ef} 3-fold higher than estimates for the last glacial period.

QUANTIFICATION AND STATISTICAL ANALYSIS

Quantification and statistical analyses were performed as described in the STAR Methods using R and other software specified in the relevant STAR Methods subsections. Unless otherwise stated, sample sizes (n) represent individual specimens for fossil material or individual animals for contemporary genomes. Exact values of n, along with what n represents, are reported in the relevant STAR Methods subsections, associated figures and figure legends, and corresponding Supplemental and Extended Data tables.

Statistical testing and model evaluation procedures, including test selection, parameter settings, summary statistics, significance thresholds, and corrections for multiple comparisons, are specified in the STAR Methods subsections corresponding to each analysis. These include non-parametric hypothesis testing using Mann–Whitney–Wilcoxon tests, multiple-testing correction using Bonferroni adjustment for window-based comparisons, permutation-based significance testing for mitochondrial FST, and axis-significance testing for ordination using Tracy–Widom tests for principal component analyses. Measures of central tendency and dispersion or precision (including mean, median, standard deviation, and confidence intervals) are reported where applicable in the results, figures, tables, and STAR Methods.

Please cite this article in press as: Westbury et al., Four centuries of commercial whaling eroded 11,000 years of population stability in bowhead whales, Cell (2026), https://doi.org/10.1016/j.cell.2026.02.022

For analyses relying on statistical assumptions, these assumptions were addressed as part of the analytical design. Non-parametric tests were used where data distributions or sample sizes did not meet parametric assumptions. Model robustness and uncertainty were evaluated using independent validation datasets and performance metrics for ecological niche modelling (including AUC and Boyce Index), downsampling and ancient DNA damage simulations to assess sensitivity of population genetic inference to coverage and damage profiles, and simulation-based inference frameworks (including Approximate Bayesian Computation and forward-time simulations) to quantify demographic change and its genomic consequences.

Supplemental figures

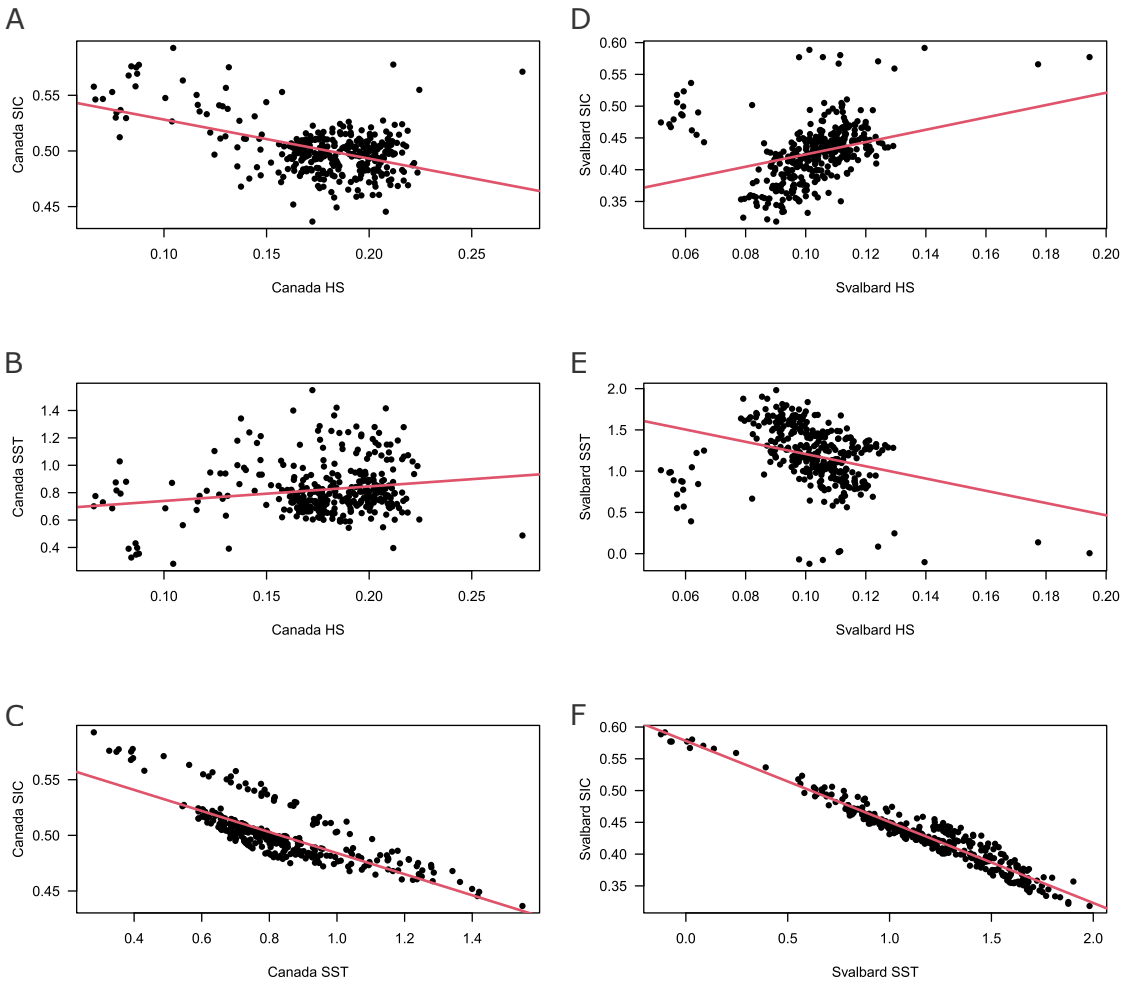

Figure S1. Correlations between HS, SIC, and SST, separated into the two study regions, Canada and Svalbard, related to Figures 2 and 3 and STAR Methods

(A–C) Canadian region: (A) sea-ice cover (SIC) against habitat suitability (HS), (B) sea-surface temperatures (SSTs) against HS, and (C) SIC against SSTs.
(D–F) Svalbard region: (D) SIC against HS, (E) SSTs against HS, and (F) SIC against SSTs.
Red line denotes the linear regression model (generalized linear model with default Gaussian family) between the two variables.

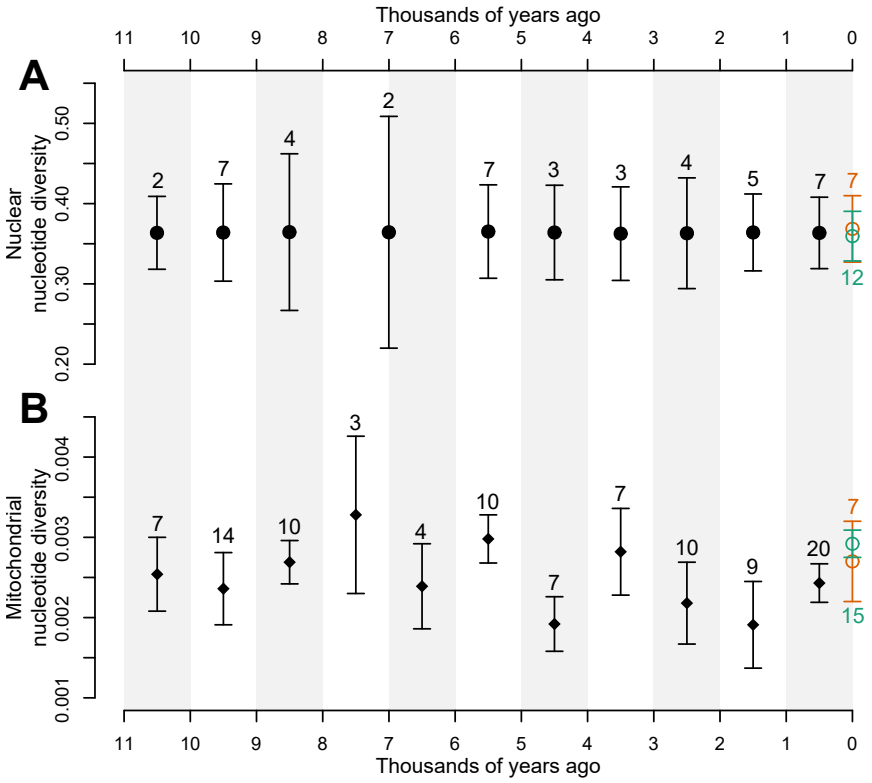

Figure S2. Holocene nucleotide diversity in bowhead whales, related to STAR Methods

(A and B) Mean (A) nuclear and (B) mitochondrial diversity are provided in 1,000-year time bins, to the exclusion of the nuclear estimates of 6,000–8,000 years ago, which were pooled into a 2,000-year time bin due to low sample size. Error bars show one standard deviation on each side of the mean. Black dots show pooled Holocene Canadian and Svalbard individuals, contemporary "ECWG" stock is in orange, and the contemporary "EGSB" stock is in green. Sample sizes for each bin are indicated. Individuals with radiocarbon dates <500 years before present (BP) that could not be accurately calibrated due to the marine-reservoir effect were added to the 0–1,000 bin.

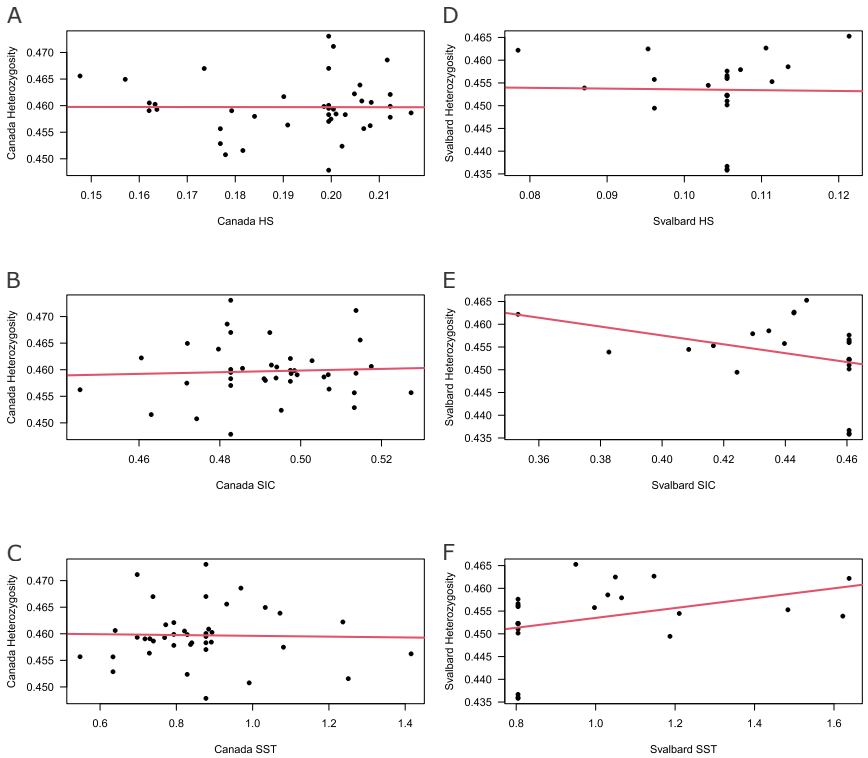

Figure S3. Correlations between genome-wide SNP heterozygosity, habitat suitability, sea ice cover, and sea surface temperature, separated into the two study regions, Canadian Arctic Archipelago and Svalbard Archipelago, related to Figures 2 and 3 and STAR Methods

(A–C) Canadian region: (A) genome-wide SNP heterozygosity against habitat suitability (HS), (B) genome-wide SNP heterozygosity against sea ice cover (SIC), and (C) genome-wide SNP heterozygosity against sea surface temperatures (SSTs).

(D–F) Svalbard region: (D) genome-wide SNP heterozygosity against HS, (E) genome-wide SNP heterozygosity against SIC, and (F) genome-wide SNP heterozygosity against SSTs.

Red line denotes the linear regression model (generalized linear model with default Gaussian family) between the two variables.

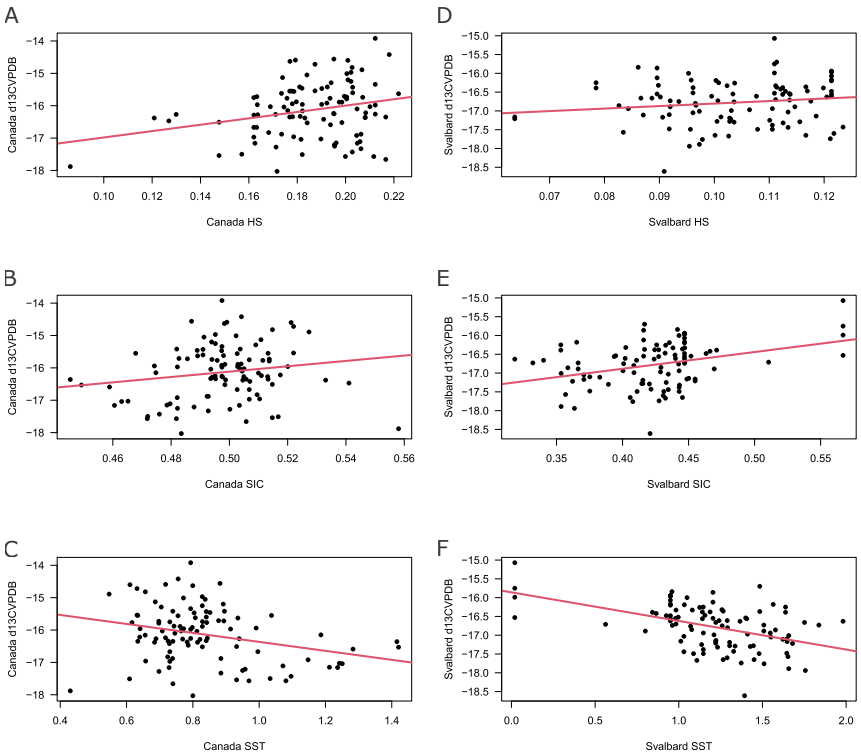

Figure S4. Correlations between δ^{13}C values and habitat suitability, sea ice cover, and sea surface temperature, separated into the two study regions, Canadian Arctic Archipelago and Svalbard Archipelago, related to Figures 2 and 3 and STAR Methods

(A–C) Canadian region: (A) δ^{13}C against HS, (B) δ^{13}C against SIC, and (C) δ^{13}C against SSTs.

(D–F) Svalbard region: (D) δ^{13}C against HS, (E) δ^{13}C against SIC, and (F) δ^{13}C against SSTs.

Red line denotes the linear regression model (generalized linear model with default Gaussian family) between the two variables.

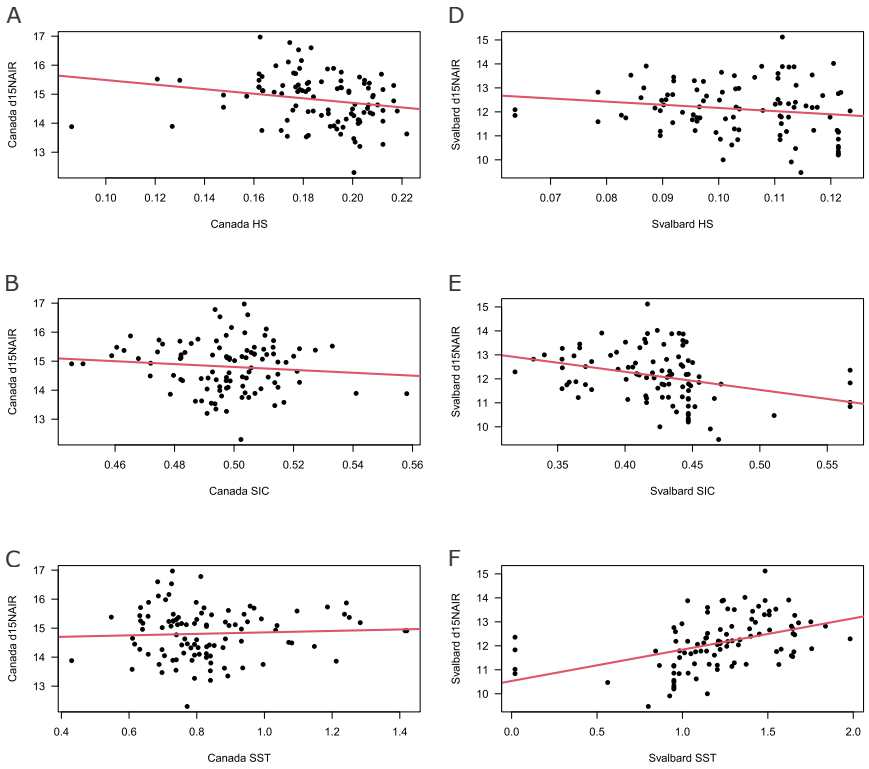

Figure S5. Correlations between δ^{15}N values and habitat suitability, sea ice cover, and sea surface temperature, separated into the two study regions, Canadian Arctic Archipelago and Svalbard Archipelago, related to Figures 2 and 3 and STAR Methods

(A–C) Canadian region: (A) δ^{15}N against HS, (B) δ^{15}N against SIC, and (C) δ^{15}N against SSTs.

(D–F) Svalbard region: (D) δ^{15}N against HS, (E) δ^{15}N against SIC, and (F) δ^{15}N against SSTs.

Red line denotes the linear regression model (generalized linear model with default Gaussian family) between the two variables.

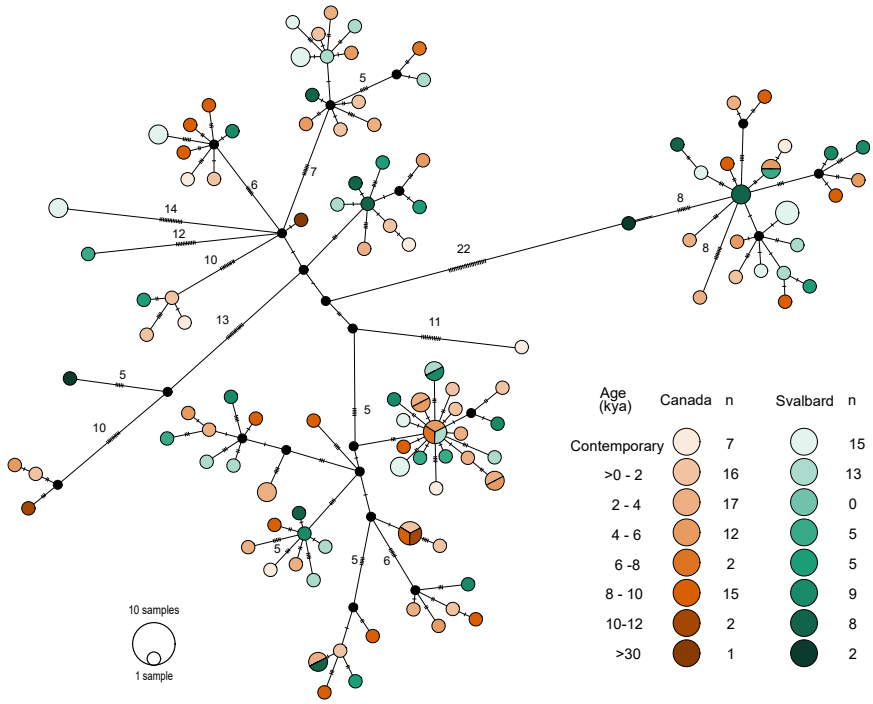

Figure S6. Haplotype network of 129 bowhead whale mitochondrial genomes (>10×), related to STAR Methods

Sample sizes for each time bin are provided and include 65 Holocene fossil sequences from Canada and 42 from Svalbard, in addition to Late Pleistocene (>30 kya) and contemporary sequences. Samples from the Canadian Arctic Archipelago are shown in orange and from the Svalbard Archipelago in green.